AMERICAN UNIVERSITY OF BEIRUT

SYNTHESIS OF CARBON INTEGRATION NETWORKS COUPLED WITH HYDRATE SUPPRESSION AND MOISTURE REMOVAL OPTIONS

by
RACHID ALIM KLAIMI

A thesis
submitted in partial fulfillment of the requirements
for the degree of Master of Science
to the Department of Chemical and Petroleum Engineering
of the Maroun Semaan Faculty of Engineering and Architecture
at the American University of Beirut

Beirut, Lebanon
May 2018

AMERICAN UNIVERSITY OF BEIRUT

SYNTHESIS OF CARBON INTEGRATION NETWORKS COUPLED WITH HYDRATE SUPPRESSION AND MOISTURE REMOVAL OPTIONS

by
RACHID ALIM KLAIMI

Approved by:

Dr. Sabla Alnouri, Assistant Professor — Advisor
Department of Chemical and Petroleum Engineering

Joseph Zeaiter
Dr. Joseph Zeaiter, Associate Professor — Member of Committee
Department of Chemical and Petroleum Engineering

Walid Saad 08 May 2018
On behalf of:
Dr. Mohammad N. Ahmad, Professor, Chairman — Member of Committee
Department of Chemical and Petroleum Engineering

Dr. Hussein Tarhini, Assistant Professor — Member of Committee
Department of Industrial Engineering and Management

Date of thesis defense: May 2, 2018

AMERICAN UNIVERSITY OF BEIRUT

THESIS, DISSERTATION, PROJECT RELEASE FORM

Student Name:
_____Klaimi_________________________Rachid_____________________________________
Last First Middle

X Master's Thesis ◯ Master's Project ◯ Doctoral Dissertation

☐ I authorize the American University of Beirut to: (a) reproduce hard or electronic copies of my thesis, dissertation, or project; (b) include such copies in the archives and digital repositories of the University; and (c) make freely available such copies to third parties for research or educational purposes.

☒ I authorize the American University of Beirut, to: (a) reproduce hard or electronic copies of it; (b) include such copies in the archives and digital repositories of the University; and (c) make freely available such copies to third parties for research or educational purposes after:

One ---- years from the date of submission of my thesis, dissertation, or project.
Two --X-- years from the date of submission of my thesis, dissertation, or project.
Three ---- years from the date of submission of my thesis, dissertation, or project.

____________________ May 09, 2018__________

Signature Date

ACKNOWLEDGMENTS

I would like to express my deepest gratitude and appreciation to my thesis advisor Dr. Sabla Alnouri for her great guidance and assistance throughout my research. Without her continuous support and involvement in every step, this work would have never been accomplished.

I would like to thank my thesis committee, Dr. Mohammad Ahmad, Dr. Joseph Zeaiter, and Dr. Hussein Tarhini for their valuable advice and encouragement at all stages of this work.

Special thanks to Dr. Patrick Linke and Dhabia Al-Mohannadi from Texas A&M university for their constructive comments and suggestions on the manuscript of my thesis paper.

Finally, I would like to thank my dearest family and friends for their great encouragement, support, and unconditional love. Their faith in my capabilities has motivated me to accomplish this work with all confidence and persistence.

AN ABSTRACT OF THE THESIS OF

Rachid Alim Klaimi for Master of Science
Major: Chemical Engineering

Title: Synthesis of Carbon Integration Networks Coupled with Hydrate Suppression and Moisture Removal Options

The excessive increase in carbon dioxide emissions through the past several decades has raised global climate change concerns. As such, environmental policy makers have been looking into the implementation of efficient strategies that would ultimately reduce greenhouse gas (GHG) emission levels, and meet strict emissions targets. As part of a national emission reduction strategy, the reduction of carbon-dioxide emissions from industrial activities has been proven to be very significant. This instigated the need for a systematic carbon integration approach that can yield cost-effective carbon integration networks, while meeting prescribed carbon dioxide emission reduction targets in industrial cities.

A novel carbon integration methodology has been previously proposed as a carbon network source-sink mapping approach using a Mixed Integer Nonlinear Program (MINLP), and was found to be very effective to devise emission control strategies in industrial cities. This work aims to further improve the design process of carbon integration networks, by coupling carbon integration networks with hydrate suppression/moisture removal options. This was found vital for the prevention of any potential hazards that are associated with the transportation of carbon dioxide in pipelines, such as hydrate formation and various corrosion effects, which may result from moisture retention. An extensive analysis of carbon capture, dehydration, inhibition, compression, and transmission options have all been incorporated into the network design process, in the course of determining cost-optimal solutions for carbon dioxide networks. The proposed approach has been illustrated using an industrial city case study that shows how the integration between different plants in a specific site could be a valuable method for carbon footprint reduction.

NOMENCLATURE

γ_d	Dehydration unit ratio of carbon dioxide emitted from energy use
γ_t	Treatment unit ratio of carbon dioxide emitted from energy use
δ_d	Dehydration unit water removal efficiency
δ_t	Treatment unit water removal efficiency
ε_d	Carbon recovery of dehydration unit
ε_t	Carbon recovery of treatment unit
ε_p	Carbon footprint parameter associated with power use
η_k	Sink k efficiency factor
θ_D	Total flow recovery of treatment unit
θ_T	Total flow recovery of dehydration unit
ρ	Density of the source stream
υ	Average velocity at source stream outlet
C_s^D	Dehydration cost parameter of flow from source s
C_s^I	Inhibition cost parameter of flow from source s
C_s^T	Treatment cost parameter of flow from source s
$C_{s,k}^{Compressor}$	Total annual compression cost using compressors
$C_{s,k}^{Pump}$	Total annual pumping cost of flow from source s to sink k
$C_{s,k}^{pipe}$	Pipe cost per unit length of connection from source s and sink k
$C_{s,k}^{Compression}$	Total annual compression cost of flow from source s to sink k
$C_{s,k}^{Dehydration}$	Total annual dehydration cost of flow from source s to sink k
$C_{s,k}^{Inhibition}$	Total annual inhibition cost of flow from source s to sink k
$C_{s,k}^{Sinks}$	Total annual processing cost of flow from source s to sink k
$C_{s,k}^{Transportation}$	Total annual transportation cost of flow from source s to sink k
$C_{s,k}^{Treatment}$	Total annual treatment cost of flow from source s to sink k

$CC^{capital}$	Capital cost of compressors
$CC^{operating}$	Operating cost of compressors
CR_k^{sink}	Sink Processing cost parameter of sink k
CRF	Capital recovery factor
D	Set of carbon dehydration technology
$D_{s,k}$	Calculated diameter of pipe between source s and sink k
$D_{s,k}^{C}$	Commercial diameter of pipe between source s and sink k
$D_{s,k,d}$	Flow from treated and dehydrated source s to sink k
F_k	Total flow into sink k
$F_{s,k}$	Total flow from source s to sink k
$F_k^{CO_2}$	Total carbon flow into sink k
G_k^{max}	Maximum flow into sink k
$H_{s,k}$	Distance between source s and sink k
K	Set of carbon sinks
L_s	Minimum total flow out of raw source s
$L_{s,k}$	Lower total flow limit from source s to sink k
m_s	Average molecular weight of source stream s
M_s	Maximum total flow out of raw source s
$M_{s,k}$	Upper total flow limit from source s to sink k
$NCRT$	Net carbon reduction target
P^{comp}	Power parameter for the compressor
P^{pump}	Power parameter for the pump
$PC^{capital}$	Capital cost of pumps
$PC^{operating}$	Operating cost of pumps
R_s	Total allocated flow from raw source s
S	Set of carbon sources
T	Set of carbon treatment technology
T_s	Temperature of source s stream outlet
$T_{s,k,t}$	Flow from treated source s to sink k

$U_{s,k}$	Flow from untreated source s to sink k
W_k^{max}	Maximum allowable water weight composition at sink k
w_s	Water weight composition of raw source s
$w_{s,d}$	Water weight composition of treated and dehydrated source s
$w_{s,t}$	Water weight composition of treated source s
w_s^u	Water weight composition of untreated source s
$X_{s,k}$	Binary associated with flow from source s to sink k
y_s	Carbon weight composition of raw source s
$y_{s,d}$	Carbon weight composition of treated and dehydrated source s
$y_{s,t}$	Carbon weight composition of treated source s
y_s^u	Carbon weight composition of untreated source s
Z_k^{min}	Minimum carbon weight composition required at sink k
$\Delta P_{s,k}$	Pressure difference between source s and sink k
$\Delta P_{s,k}^{pipe}$	Pressure drop between source s and sink k

CONTENTS

Appendix

ILLUSTRATIONS

TABLES

CHAPTER I

INTRODUCTION

The adverse environmental, economic and social impacts of global warming and climate change have resulted in extensive global efforts for greenhouse gas (GHG) emissions reduction. In 2015, carbon dioxide (CO_2) emissions have reached more than 70% of the total annual global GHG emissions estimated by 49.1 billion tons of CO_2-equivalent (Olivier et al., 2016). According to the BP Statistical Review of World Energy (2017), the top 10 carbon emitting countries, led by China, USA and Russia, are responsible for more than 68% of global CO_2 emissions (Dong et al., 2018). Since carbon dioxide is the largest contributor in the increase of greenhouse gas emissions, scientists and policy makers have agreed on limiting CO_2 production, especially that this trend is expected to continue with the growth in population that would reach 9 billion people by 2050 (Metz et al., 2005). However, the target of carbon footprint reduction consists an important challenge for the industrial sectors due to their extensive rely on energy from different types of fossil fuels, such as coal, natural gas, and oil. The International Energy Agency (IEA) data, for 2015, showed that coal combustion was responsible for about 46% of the global CO_2 emissions from fossil fuels combustion, while about 34% of carbon dioxide was emitted as a result of energy production from natural gas. However, a remarkable increase in the use of natural gas has been witnessed in the few past years, especially in USA and China, due to their increase in energy consumption. For instance, around 81% of the total required energy in the United States comes from fossil fuels. It was reported that US electricity was produced, in 2015, from almost an equal amount of coal (33.2%) and natural gas (32.7%). Therefore, the Environmental Investigation Agency (2016) expected that CO_2 emissions from natural gas combustion will surpass those from coal combustion in the next few years (Olivier et al., 2016).

Although carbon dioxide does exist naturally, the majority of CO_2 present in nature is due to human consumption of fuels for power production and transportation, or its release as a by-product from various industrial and agricultural activities. Carbon dioxide emissions differ between developed and developing countries. For instance, statistics showed that Canada and the United States had CO_2 emissions of 19 and 16.5 metric tons/capita in 2015, respectively, while Brazil and India's emissions were not more than 2.5 and 2 metric tons of CO_2/capita, respectively (Olivier et al., 2016). In order to avoid dangerous climate change effects, the Intergovernmental Panel on Climate change (IPCC) suggested a CO_2 reduction target of 80% for developed countries, and 30% for developing countries, to be achieved by 2050 (Metz et al., 2005). In Lebanon, the case is much similar, and in accordance to the agreement held in Paris by over 190 countries in December 2015, it has set a target of 15% CO_2 reduction by 2030 with a commitment to reducing 30% of its emissions subject to financial availability, capacity building, and technical support (UNDP, 2016). On the other hand, the European Union (EU) has committed to the Kyoto protocol running from 2013 to 2020. As a result, the EU has been planning on reducing their GHG and carbon emissions by 20% in 2020, with a long-term emission reduction goal of 80-95%, by

2050 (European Commission, 2016). Today, some EU countries are worried about asking them to increase their reduction targets after the Brexit. Based on the calculations made by analysts at Thompson Reuters Point Carbon, an extra 1.1 to 2% reduction may be added to the target of the union's countries if Britain's share were to be redistributed evenly (Darby, 2016). For countries like Qatar, which is a member in the Gulf Cooperation Council (GCC) and a major oil and gas producer, its economy is mainly dependent on the oil and gas sector. GCC member states hold 23.6% of the world's proven gas reserves and around 40% of the world's proven oil (Reiche, 2010). This places Qatar on the very top of the CO_2 producing countries in the world, with an average of 38.52 metric tons CO_2/capita in 2016 (World Data Atlas, 2016). Figure (1) below shows the distribution of main CO_2 emission sectors in Qatar in 2016 where stationary sources are responsible for more than 70% of the total country's emissions.

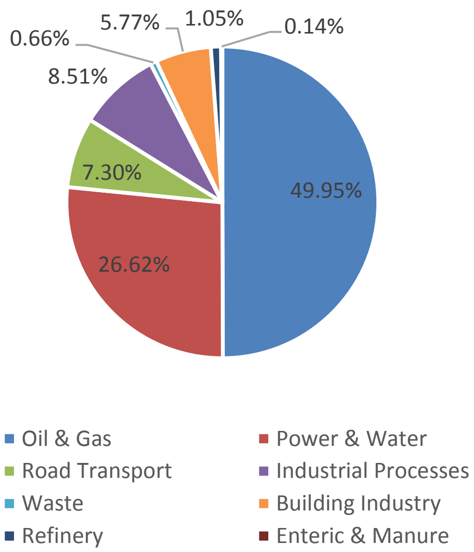

Figure 1: Qatar Main CO_2 Emission Sectors

Carbon integration is a new method for the systematic identification of optimal choices for the reduction of carbon emissions through the integration of Carbon Capture, Storage and Utilization (CCUS) options across different industries and processes. The method is based on the structural optimization of the CCUS allocation networks and has been extended to explore interactions with heat and energy integration problems (Al-Mohannadi and Linke, 2016, Al-Mohannadi et al., 2016) as well as simultaneous decision making on natural gas monetization, renewable energy integration and CCUS selection (Al-Mohannadi et al., 2017). In the CCUS networks, a carbon dioxide source stream passes through several stages of treatment, compression, and transportation before being processed into the potential sinks. Pipeline transport is the main method to transport carbon to the storage sites in CCUS networks. However, the presence of moisture in the captured carbon streams has a major impact on the CO_2 pipeline. One of the main hazards associated with the presence of moisture is the formation of carbon hydrates which results in destroying the equipment and blocking the pipeline (Zhang et al., 2016). This will lead to a production stoppage, in addition to higher costs of hydrate prevention or removal, and other environmental hazards (Bavoh et al., 2016). The existence of free water in CO_2 streams can also cause the electrochemical corrosion of the pipeline inner wall which threatens the security and stability of the pipeline (Carroll, 2003). Moreover, the moisture presence can cause pressure drops resulting in two-phase flow and liquid slugs in the pipeline (Abbas et al., 2013, Aspelund and Jordal, 2007). Therefore, accounting for the presence of water vapor which may affect the piping systems was found vital for the prevention of any potential hazards that are associated with the transportation of carbon dioxide in pipelines, such as hydrate formation and various corrosion effects, that result from moisture retention.

This work aims to present a new approach of carbon integration coupled with hydrate suppression and moisture removal options. Carbon emissions reduction was addressed by many researches that studied the problem and suggested several methods for carbon reduction within single plants. However, the approach presented in this paper is applied on a real industrial city located in Qatar to show how the collaboration and integration between different plants within a specific site could introduce a new perspective of carbon footprint reduction in order to achieve the reduction targets set out by the country.

CHAPTER II

LITERATURE REVIEW

A. Carbon Dioxide Integration

Various methods for carbon footprint reduction replace energy sources with other alternatives, such as renewables, nuclear energy and biomass. For instance, Said et al. (2018) have predicted the UAE's future energy mix by introducing renewable energy systems to satisfy the imposed target of CO_2 emissions reduction. Although the proposed study of implementing photovoltaic and concentrated solar power plants is expensive, since the shift into renewable energy is challenging compared to the fossil fuels based technologies, it was found that a carbon reduction of 7% annually is achievable by increasing the contribution of renewable energy mix up to 2030 (Said et al., 2018). Recka and Scasny (2018) have studied the effect of nuclear energy deployment on carbon reduction targets in the Czech Republic up to 2050. They found that declining coal usage in all sectors of the economy and replacing it with advanced technologies with higher efficiencies will result in a total carbon emissions reduction by 51% of the 2015 level in 2050 (Rečka and Ščasný, 2018). On the other hand, Furubayashi and Nakata (2018) conducted a study to investigate the effect of using different types of waste wood biomass as a fuel source, for electricity production, on CO_2 emissions reduction in Japan. Their study showed that around 70% of CO_2

reduction can be achieved in this sector depending on the type of biomass used (Furubayashi and Nakata, 2018). However, even though fossil fuel energy replacement with renewable energy sources might be appealing for the industry, this act of adaptation may be slow due to the wide use of fossil fuels in the current industries.

Carbon reduction and energy planning problems have been addressed through various graphical methods. For instance, the Graphical Carbon Emission Pinch Analysis (CEPA) method has been applied by Atkins et al., (2010), to reduce carbon emissions from a New Zealand electricity sector. This energy integration tool which was first developed by Tan and Foo (Tan and Foo, 2007) has been successfully applied on macro-level regional emissions planning and targeting through the usage of renewable energy sources that can minimize the carbon emissions to the specified targets while meeting the energy demand (Atkins et al., 2010). Perry et al., (2008), have extended a method known as the total site methodology for heat integration to allow for the reduction of carbon emissions from energy users (Perry et al., 2008). Munir et al., (2012), have presented a new process integration technique to achieve minimum carbon targets, consisting of a graphical pinch method with a set of heuristics for emissions reduction based on source-sink network (Munir et al., 2012). Moreover, Carbon Capture and Storage (CSS) in the form of graphical methods have also been used for carbon footprint reduction associated with energy use. For instance, Ooi et al., (2013), have proposed a graphical Carbon-Constrained Energy Planning (CCEP) method, which is a new research area that addresses carbon emissions reduction issues during energy planning stage (Ooi et al., 2013).

Although carbon reduction and energy planning problems have been addressed through different graphical methods, their wide applicability might be limited due to the over-simplifications required by some of the methods. Therefore, many alternative mathematical approaches have been developed, as a mean to improve graphical approaches. Shenoy and Shenoy, (2012), have looked to the problem from another perspective by including carbon capture and storage (CCS) as an interceptor, and investigated energy integration options with carbon removal. They have applied a mixed integer linear program (MILP) for hybrid targeting/optimization (Shenoy and Shenoy, 2012).

Emission reduction targeting through energy planning (or energy integration) have also been investigated. Some of the applied methods investigated the usage of less energy with more efficient designs by reducing carbon dioxide emitted from combustion processes, while others aimed towards cutting the amount of external energy sources, and incorporating energy recovery from waste heat. For instance, Chae et al. (2010) have addressed the interplant energy integration for waste heat reduction, while Stijepovic and Linke (2011) have looked at the problem of energy recovery and re-use from multiple plants (Chae et al., 2010, Stijepovic and Linke, 2011).

Nevertheless, it is worth to mention that all these methods were just applied to reduce the carbon emissions without dealing with the inevitable produced carbon. A case study for carbon dioxide capture in an industrial park with multiple CO_2 sources has been discussed by Norstebo et al. (Nørstebø et al., 2012). They have focused on the carbon capture facility with varying volumes and concentrations of carbon dioxide taking into consideration CO_2 taxation as a way for emissions reduction. This attempt of carbon reduction considered the flow of CO_2 from the carbon sources to a single capture unit without allocating them to the target sinks. Kwinana Australia Beers (van Beers, 2006) has also demonstrated the placement of carbon dioxide in processes of an Eco-Industrial Park. However, this demonstration also did not address the systematic matching of the captured CO_2 streams with the utilization sinks in the industrial park.

B. Moisture Effects on CO_2 Transport

Generally, the three common methods for transporting carbon dioxide are tanker transportation, ship transportation, and pipeline transportation. Tanker transportation is the most expensive among the three methods of transmission. Therefore, it is usually used for small volumes and short distances, such as in small oil fields for CO_2 flooding experiments. Ship transportation is only applicable in the seas and rivers areas, and the storage equipment should bear low temperature and high-pressure conditions. On the other hand, pipeline transportation is suitable for transferring large capacities of CO_2 over long distances in reasonable costs (Zhang et al., 2016). Therefore, numerous researches on the transportation of carbon dioxide showed that pipeline transportation is the most economic method for large scale of CO_2 (Prah and Yun, 2017). However, CO_2 transport in pipelines is usually associated with several hazards, such as formation of CO_2 hydrates, that may result in inefficient transmission of carbon dioxide.

CO_2 hydrate is an ice-like crystalline compound that belongs to the clathrate hydrate group that forms when sufficient amounts of carbon dioxide and water are combined at suitable temperature and pressure conditions. Formation of CO_2 hydrates takes place by trapping carbon dioxide molecules in water cavities as guest molecules, resulting in a structure (I) hydrate crystals (Prah and Yun, 2018). These crystals will most likely cause the blockage of the pipelines, resulting in various operational and safety issues. Therefore, the presence of moisture in the captured CO_2 streams is a major challenge for the transport of carbon dioxide from sources to sinks, and it should be managed in order to prevent CO_2 hydrates formation in the pipelines. There are four main techniques for hydrate formation prevention:

- Carbon dehydration using different technologies
- Maintaining high operating temperatures
- Maintaining low operating pressures
- Injection of specific inhibitors for hydrate prevention

Several technologies that are suitable for CO_2 dehydration already exist. Some of these techniques do not achieve low moisture content, but they are mainly used for their easy application and low cost, such as compressor inter-stage cooling. Moreover, some of the conventional dehydration technologies face some challenges, such as the effect of impurities present in the CO_2 stream on the dehydration process, that prevent them from being deployed in full-scale. Therefore, molecular sieving and triethylene glycol (TEG) systems are the most recommended technologies due to their high moisture removal and relatively low operation costs (Kemper et al., 2014). It was also reported that the presence of some impurities, such as NO_x and SO_x will increase the capital cost of these technologies by around 7% with no significant change in the operational cost (Kemper et al., 2014). Concerning water threshold for hydrate prevention, Benson et al. (2012) have suggested that the maximum allowable moisture content must be in the range of 50-500 ppm, which is achievable using both technologies (Benson et al., 2012, Ussiri and Lal, 2017).

Another method of hydrate prevention is controlling the temperature and pressure of CO_2 during its transmission from the source to the sink. Zhang et. al (2016) have conducted a research on hydrate formation in gaseous phase CO_2 pipeline transportation. They found that at a pressure of 1.45 MPa, CO_2 hydrates start forming at a temperature of around 5^{o}C. Therefore, it is always recommended to transport carbon dioxide at high temperatures or low pressures in order to avoid the formation of these hydrates. However, this technique is not always applicable, since, carbon sinks may be operating at high pressures, such as in geological sequestration. In this case, carbon dioxide pressure must meet its sink requirement, so that it must be transported at a high pressure. In their study, Zhang et al. (2016) have also investigated the effect of impurities on hydrate formation. They found that a small amount of impurities has almost little effect on CO_2 hydrate formation. However, when the pressure in the pipelines is between 3.5 MPa to 4.5 MPa, the small amount of impurities may result in a slight increase in the temperature at which hydrates form, and CO_2 hydrate formation temperature will reach 10^{o}C (Zhang et al., 2016). Yang et al. (2013) have investigated the flow direction of carbon dioxide flowing through cooled porous media on hydrate formation and dissociation. They found that carbon hydrate can be formed more easily in a vertically upward flow than a downward flow. This can be related to the effect of gravity which allows the moisture to be easily driven away, in a downward flow, missing the chance of a sufficient contact with carbon dioxide (Yang et al., 2013).

Hydrate inhibitors injection is the most common method used to prevent the formation of hydrates in pipelines (Kelland et al., 2013). Before 1990s, thermodynamic hydrate inhibitors (THIs), such as glycol, salts and alcohols, were the first type of inhibitors to be used due to their ability of increasing the pressure and decreasing the temperature of hydrate formation. However, large concentrations of THIs are usually required (40-60 wt.%), resulting in a higher inhibition cost (Sloan Jr and Koh, 2007). Low dosage hydrate inhibitors (LDHIs) were then introduced with a main advantage of being effective at very low concentrations (below 1 wt.%). These inhibitors are divided into two groups: kinetic hydrate inhibitors (KHIs) which slow down the formation of hydrate crystals by retarding nucleation, and anti-agglomerates (AAs) which work on dispersing the small hydrate crystals and preventing their agglomeration (Kelland, 2006). Bavoh et al. (2017) have studied the inhibition effect of several amino acids with different concentrations using the isochoric T-cycle method and found that glycine has the highest inhibition effect at a concentration of 10 wt.%. Their work ensured that the strength of amino acids inhibition lies in their ability of reducing water activity in hydrate formation resulted from hydrogen bonding with water molecules (Bavoh et al., 2017). Water-soluble polymers, such as PVCap and PVP, are another type of KHIs which are most commonly used for hydrate suppression. However, the main problem of these inhibitors is their poor biodegradability. Therefore, Roosta et al. (2016) have focused on developing kinetic inhibitors which are environmentally friendly by investigating the inhibition properties of several new amino acids for hydrate suppression in carbon dioxide-water systems. The results of their experimental work showed that L-Histidine with charged side chain and high net charge is the most effective amino acid in preventing the formation of CO_2 hydrates. Moreover, the results showed that the inhibition effect increases with the increase in the concentration and hydrophobicity of the inhibitor (Roosta et al., 2016).

All the mentioned studies were focusing on the enhancement of CO_2 transportation through the prevention of CO_2 hydrate formation in pipelines. However, Prah and Yun (2018) have turned the risk of hydrate formation into a new method of CO_2 transportation. This application consists of a rapid entrapment of carbon dioxide through hydrate formation at mild temperatures and pressures, followed by a release of the captured gas through hydrate decomposition. They have found that transferring CO_2 in the form of hydrate slurry reduces the required energy input, resulting in a reduction in transportation cost. Moreover, the injection of anti-agglomerates enhances the gas transfer by reducing the liquid-gas interfacial tension and the interfacial resistance to the diffusion and solubility of gas molecules (Prah and Yun, 2018, Aman and Koh, 2016). Another problem caused by the presence of free water in CO_2 pipelines is corrosion. Wet CO_2 is characterized by a corrosive nature which threatens its transport system integrity. Therefore, it is very important to study the different methods that prevent the occurrence of this hazard. Carbon steel is commonly used for most CO_2 pipelines due to its high corrosion resistance. However, it would be expensive, from an economic perspective, to build a pipelines system with this type of steel (Buit et al., 2011). Thus, carbon dehydration would be an alternative method which is widely used in the industries for such purposes. Unfortunately, the present literature lacks clarity on the carbon dryness requirements which is undesirable, since it is important to have a standard moisture content that ensures a cost-effective carbon transport. Therefore, Xiang et al. (2012) have conducted a research to provide some basic input on the upper limit of moisture content for supercritical CO_2 pipeline transport. The results of their study strongly support the recommended moisture limit of 500 ppm proposed by DYNAMIS (Hydrogen and Electricity Production with Carbon Dioxide Capture and Storage) project (Xiang et al., 2012, De Visser et al., 2008), while the Barendrecht CO_2 storage correspondence have suggested a tighter limit of 40 ppm (Buit et al., 2011). Regardless of all the different moisture limits reported in the literature, all the researchers have agreed that drying captured CO_2 reduces the flexibility of carbon chain, and costs both energy and money. Therefore, the moisture content limit should not be more stringent than necessary. Olvera-Martinez et al. (2015) have looked to the problem from another perspective, since they have studied the influence of turbulent flow on the performance of corrosion inhibitors in CO_2 pipelines. Based on their study, it was found that, at constant concentration, the inhibition efficiency is dependent on turbulent flow conditions which is associated with the diffusion of inhibitor molecules from the bulk of the solution to the surface of the steel (Olvera-Martínez et al., 2015).

The above studies consider the problems of hydrate formation and corrosion in CO_2 pipelines separately. Therefore, this work will present a new approach that combines the two hazards with the process of carbon integration in industrial parks to develop cost optimal carbon dioxide networks. The methodology and mathematical models are presented in the next chapters.

CHAPTER III

METHODOLOGY

The overall approach adapted in this study builds on the work of Al-Mohannadi and Linke (Al-Mohannadi and Linke, 2016). A source is defined as an emission point of a process in a plant within the industrial city. Sources could be either a process emitted or purged sub-stream, and they can have different flowrates, compositions, and parameters. On the other hand, a sink is defined as a unit that consumes, intakes, converts, or stores carbon dioxide. Sinks could be biological or geological sequestration outside the industrial city or processes within the studied city. An example about biological sequestration is the use of CO_2 in algae growth, while geological sequestration could be saline storage or enhanced gas/oil or coal bed recovery. Table (1) below summarizes the different hydrate suppression and moisture removal options that were previously discussed along with their advantages and disadvantages. Carbon dehydration and inhibitors injection are the two methods that will be considered in this work due to their easy application, high efficiency, and low cost. However, some types of inhibitors may affect the carbon sinks negatively. The other two methods are temperature and pressure control that will not be considered in this work, since their applicability depends on the carbon sinks pressure and temperature conditions.

Table 1: Hydrate Suppression and Moisture Removal Options

Option	Advantages	Disadvantages	Considered in this Work
Dehydration	- Easy application - High efficiency - Low cost		Yes
Pressure Control	- Moderate efficiency	- Not always applicable	No
Temperature Control	- Moderate efficiency	- Not always applicable - Energy added cost	No
Inhibitors Injection	- Easy application - High efficiency - Low cost	- Might have side effects on carbon sinks	Yes

The amended approach consists of three different options for carbon allocation from sources to sinks. A source stream might be directly used as a carbon diluted source called “untreated”, or it might undergo a carbon removal and it is called “treated” in this case, while the third option is to pass through a carbon removal and dehydration units to be called a “treated and dehydrated” stream. The first two types of sources are exposed to hydrate formation and corrosion problems, since their water content is above the standard threshold. Therefore, an injection of inhibitors is found to be a critical solution to prevent the occurrence of these problems. Each sink could accept all the types of sources as well as mixtures of them. Hence, when different types of streams from the same raw source are allocated to the same sink, they can be transported in a common interconnecting pipeline to reduce the delivery cost. Moreover, all the sources require a change in pressure in order to meet sinks pressure requirements and overcome pressure drop in the transmission lines. An illustration of the carbon connections from a single source is shown in Figure (2).

As mentioned above, one of the options requires carbon dehydration after its capture from the raw source. Hence, the following additional information are required for this work:

- Dehydration units' costs which are also dependent on the technology chosen, whether using solid/liquid desiccants or membrane technologies.
- Dehydration units' water removal efficiency which can be determined from literature.
- Dehydration units' carbon removal parameter and carbon emission parameter which are, similarly, dependent on the dehydration units' recovery and energy use, respectively.
- Hydrate formation and corrosion inhibition costs.

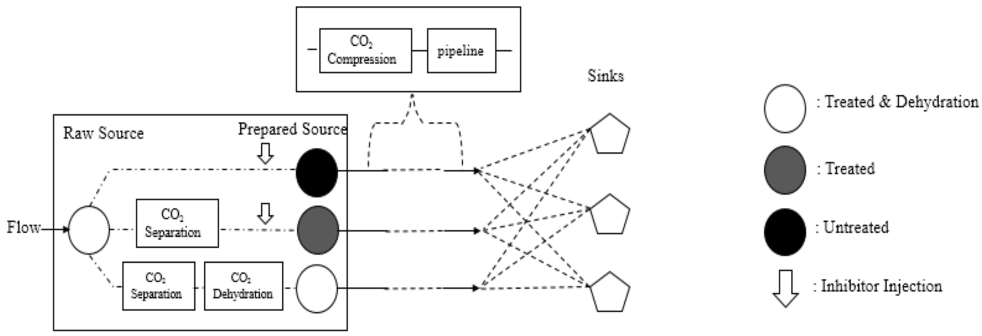

Figure 2: Single-Source Representation

CHAPTER IV

MATHEMATICAL FORMULATION

The optimization problem is defined as follows:

Given is an industrial park with a number of carbon emission sources, with known flowrate, composition, pressure and temperature, that should be allocated to potential existing sinks with known capacity, minimum carbon requirement, maximum allowable moisture content, pressure and temperature, in addition to the distances between all sources and sinks. The aim is to design a carbon integration network with the minimum cost to achieve the carbon integration reduction target. A carbon integration network consists of one or several source streams, carbon capture and dehydration units, compression units, pipelines and sink processes.

Following from the above, a number of sets was defined as a basis for the problem formulation:

S $\{s|s=1, 2, 3, \ldots, N_{sources}|$ S is a set of carbon sources$\}$

K $\{k|k=1, 2, 3, \ldots, M_{sinks}|$ K is a set of carbon sinks$\}$

T $\{t|t=1, 2, 3, \ldots, T_{max}|$ T is a set of carbon treatment technology$\}$

D $\{d|d=1, 2, 3, \ldots, D_{max}|$ D is a set of carbon dehydration technology$\}$

Figure (3) shows the CO_2 network representation with multiple sources and sinks.

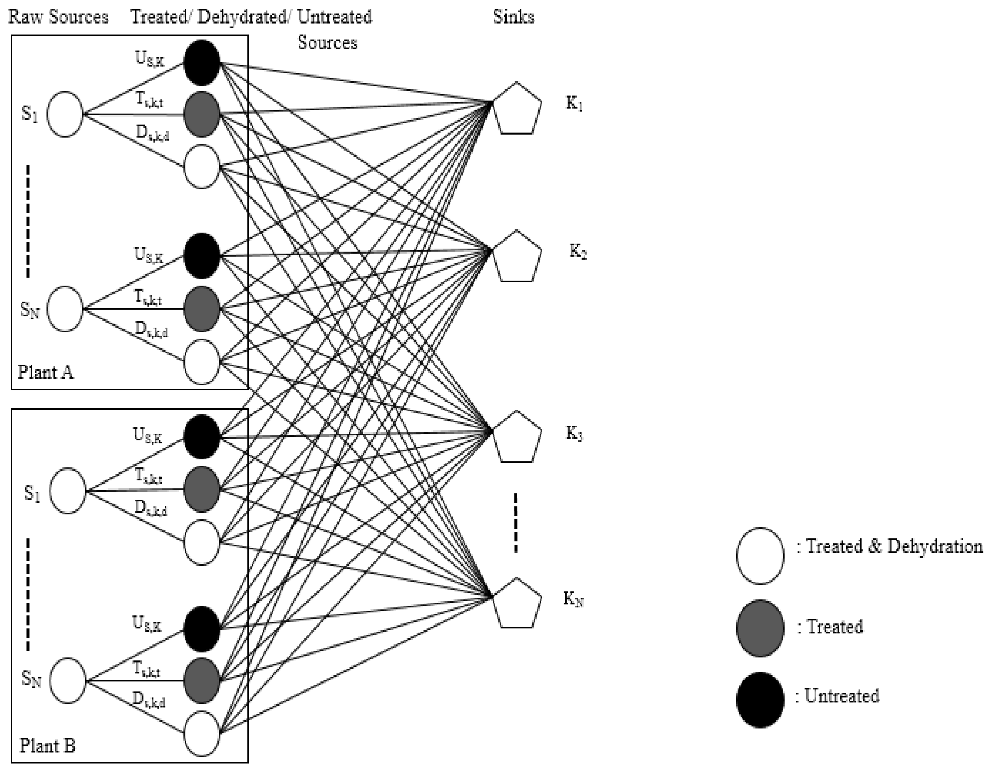

Figure 3: Source-Sink Matching

A raw source s located in a specific plant has a flowrate (R_s), carbon composition (y_s), and water composition (w_s). It can be allocated to a sink k as an untreated source flow ($U_{s,k}$), a treated source flow ($T_{s,k,t}$), or a treated and dehydrated source flow ($D_{s,k,d}$). The untreated source is a split of the main raw stream with the same carbon and water compositions of y_s and w_s, respectively. The treated source has a carbon composition ($y_{s,t}$) based on the carbon removal efficiency ε_t of the treatment technology t, and a water composition ($w_{s,t}$). The treated and dehydrated source has a carbon composition ($y_{s,d}$) and a water composition ($w_{s,d}$) based on the carbon and water removal efficiencies of the treatment and dehydration units. The raw source flow (R_s)

can be allocated between a lower limit set by the user and an upper limit which is the maximum available source flow:

$$L_s \leq R_s \leq M_s \;\; \forall\, s \epsilon S \tag{1}$$

To ensure that the flow does not exceed the available capacity, a total and component mass balances around each source s and sink k are inevitable. The total flow recovery of the treatment unit and the dehydration unit can be calculated using equations (2) and (3), respectively. The treatment unit recovery (θ_{Ts}) of source s is the summation of the carbon composition in source s (y_s) multiplied by the carbon removal efficiency (ε_T) and the water composition in source s (w_s) multiplied by the water removal efficiency of the treatment unit (δ_T), while the recovery of the total flow that undergoes a treatment and dehydration (θ_{Ds}) is the carbon composition in source s (y_s) multiplied by the carbon removal efficiency (ε_T) and carbon recovery of the dehydration unit (ε_D) added to the water composition in source s (w_s) multiplied by the water removal efficiencies of the treatment and dehydration units (δ_T and δ_D).

$$\theta_{Ts} = y_s \varepsilon_T + w_s \delta_T \tag{2}$$

$$\theta_{Ds} = y_s \varepsilon_T \varepsilon_D + w_s \delta_T \delta_D \tag{3}$$

The total flow allocated from source s (R_s) is equal to the summation of all the untreated streams from source s ($U_{s,k}$) plus the summation of all the treated streams from source s ($T_{s,k,t}$) multiplied by the treatment unit recovery (θ_{Ts}) and the summation of all the treated and dehydrated streams from source s ($D_{s,k,d}$) multiplied by the recovery factor of treatment and dehydration (θ_{Ds}), as shown in equation (4) below:

$$R_s = \sum_{k\epsilon K} U_{s,k} + \sum_{k\epsilon K} \sum_{t\epsilon T} \theta_{Ts}\, T_{s,k,t} + \sum_{k\epsilon K} \sum_{d\epsilon D} \theta_{Ds}\, D_{s,k,d};\ \forall\ s\epsilon S \qquad (4)$$

The total allocated flow from source s (R_s) multiplied by the raw source carbon composition (y_s) represents the total allocated carbon dioxide flow from source s. The total allocated carbon dioxide flow is the summation of all the untreated streams from source s ($U_{s,k}$) multiplied by their carbon composition (y_s^u), added to the summation of all the treated streams from source s ($T_{s,k}$) multiplied by their carbon composition ($y_{s,t}$) and the treatment unit recovery (θ_{Ts}), and the summation of all the treated and dehydrated streams from source s ($D_{s,k}$) multiplied by their carbon composition ($y_{s,d}$) and the dehydration unit recovery (θ_{Ds}). The component mass balance for carbon dioxide is shown in equation (5).

$$R_s y_s = \sum_{k\epsilon K} U_{s,k}\, y_s^u + \sum_{k\epsilon K} \sum_{t\epsilon T} \theta_{Ts}\, T_{s,k,t} y_{s,t} + \sum_{k\epsilon K} \sum_{d\epsilon D} \theta_{Ds}\, D_{s,k,d} y_{s,d};\ \ \forall\ s\epsilon S \quad (5)$$

Similarly, for the water component mass balance, the same equation is applied by replacing all the compositions and factors of carbon with those of water, as shown in equation (6).

$$R_s w_s = \sum_{k\epsilon K} U_{s,k}\, w_s^u + \sum_{k\epsilon K} \sum_{t\epsilon T} \theta_{Ts}\, T_{s,k,t} w_{s,t} + \sum_{k\epsilon K} \sum_{d\epsilon D} \theta_{Ds}\, D_{s,k,d} w_{s,d};\ \ \forall\ s\epsilon S \quad (6)$$

The total flow allocated in a sink k (F_k) is equal to the summation of all the untreated streams to sink k ($U_{s,k}$) plus the summation of all the treated streams to sink k ($T_{s,k}$) multiplied by the treatment unit recovery (θ_{Ts}) and the summation of all the treated and dehydrated streams to sink k ($D_{s,k,d}$) multiplied by the recovery factor of treatment and dehydration (θ_{Ds}), as shown in equation (7) below:

$$F_k = \sum_{s\epsilon S} U_{s,k} + \sum_{s\epsilon S} \sum_{t\epsilon T}\ \theta_{Ts}\, T_{s,k,t} + \sum_{s\epsilon S} \sum_{d\epsilon D} \theta_{Ds} D_{s,k,d}\ ;\ \forall\ k\epsilon K \quad (7)$$

The total flow allocated at sink k multiplied by the minimum carbon composition required at sink k (Z_k^{min}) is equal to the minimum carbon flow required at sink k. This flow should be less than or equal to the actual carbon flow to sink k which is equal to the summation of all the untreated sources to sink k ($U_{s,k}$) multiplied by their carbon composition (y_s^u) added to the summation of all the treated sources to sink k ($T_{s,k}$) multiplied by their carbon composition ($y_{s,t}$) and the total flow recovery (θ_{Ts}), and the summation of all the treated and dehydrated sources to sink k ($D_{s,k}$) multiplied by their carbon composition ($y_{s,d}$) and the total flow recovery (θ_{Ds}),, as shown in equation (8) below:

$$F_k Z_k^{min} \leq \sum_{s\epsilon S} U_{s,k}\, y_s^u + \sum_{s\epsilon S} \sum_{t\epsilon T} \theta_{Ts}\, T_{s,k,t}\, y_{s,t} \sum_{s\epsilon S} \sum_{d\epsilon D} \theta_{Ds}\, D_{s,k,d}\, y_{s,d}\ ;\ \forall\ k\epsilon K \quad (8)$$

The total flow allocated at sink k multiplied by the maximum water composition allowed at sink k (W_k^{max}) is equal to the maximum water load allowed at sink k. This load should be greater than or equal to the actual water flow to sink k which is equal to the summation of all the untreated sources to sink k ($U_{s,k}$) multiplied by their water composition (w_s^u), added to the summation of all the treated sources to sink k ($T_{s,k}$) multiplied by their water composition ($w_{s,t}$) and the summation of all the treated and dehydrated sources to sink k ($D_{s,k}$) multiplied by their water composition ($w_{s,d}$), as shown in equation (9):

$$F_k W_k^{max} \geq \sum_{s\epsilon S} U_{s,k}\, w_s^u + \sum_{s\epsilon S} \sum_{t\epsilon T} \theta_{Ts}\, T_{s,k,t}\, w_{s,t} + \sum_{s\epsilon S} \sum_{d\epsilon D} \theta_{Ds}\, D_{s,k,d}\, w_{s,d};\ \forall\ k\epsilon K \quad (9)$$

All the untreated streams have the same carbon dioxide and water concentrations of the raw source:

$$y_s^u = y_s;\ \forall\ s\epsilon S \quad (10)$$

$$w_s^u = w_s;\ \forall\ s\epsilon S \quad (11)$$

Any source could be connected to any sink as long as it achieves the composition requirements (Z_k^{min}) and (W_k^{max}), and falls under the capacity limit (G_k^{max}) as described in equations (12)- (14):

$$F_k \leq G_k^{max};\ \forall\ k\epsilon K \tag{12}$$

$$y_k \geq Z_k^{min};\ \forall\ k\epsilon K \tag{13}$$

$$w_k \leq W_k^{max};\ \forall\ k\epsilon K \tag{14}$$

In general, all sources could be connected to all sinks. However, from an optimization point of view, it is recommended to not have connections with very small capacities due to the additional costs resulted from the fixed costs in the correlations. Therefore, binary variables ($X_{s,k}$) that are defined below were added to express a minimum flow constraint, and, consequently, avoid unfeasible small connections. Hence, the summation of the untreated, treated, and treated and dehydrated flow from source s to sink k should be within a lower ($L_{s,k}$) and an upper limit ($M_{s,k}$) multiplied by the corresponding binary variable ($X_{s,k}$), as shown in equation (15).

$$L_{s,k}\, X_{s,k} \leq\ T_{s,k,t} +\ U_{s,k} +\ D_{s,k,d}\ \leq\ M_{s,k}\, X_{s,k}\ \ \forall\ s\epsilon S, k\epsilon K, t\epsilon T, d\epsilon D \tag{15}$$

Since carbon dioxide footprint reduction is the main aim of this study, a net capture constraint was added in order to achieve the targets set on the city. Hence, the net capture must be greater than or equal to the net carbon reduction target NCRT, as shown in equation (16):

$$Net\ Capture\ \geq NCRT \tag{16}$$

Where, NCRT represents the net capture reduction target which is set by the user, and the net capture is defined by the difference between the total allocated CO_2 and total CO_2 emitted to the atmosphere. The summation of all the allocated carbon dioxide flows (F_k^{CO2}) multiplied by a factor of $(1-\eta_k)$, where η_k is the sink efficiency, represents the total allocated carbon dioxide. The total emitted CO_2 is the summation of:

1) Carbon emitted from the treatment unit which is equal the summation of the treated streams ($T_{s,k,t}$) multiplied by the treatment unit recovery (θ_{Ts}), carbon concentration ($y_{s,t}$) and the parameter γ_t which is the total amount of CO_2 emitted from the energy use of the treatment unit.

2) Carbon emitted from the dehydration unit which is equal the summation of the treated and dehydrated streams ($D_{s,k,t}$) multiplied by the dehydration unit recovery (θ_{Ds}), carbon concentration ($y_{s,d}$) and the addition of the parameters γ_t and γ_d ,where γ_d is the total amount of CO_2 emitted from the energy use of the dehydration unit.

3) Carbon emitted from the power use which is equal to the summation of all the allocated carbon dioxide flows (F_k^{CO2}) multiplied by the power use parameter ε_p.

$$Net\ Capture = \sum F_k^{CO2}\,(1-\eta_k) - \sum \theta_{Ts} T_{s,k,t}\, y_{s,t}\gamma_t - \sum \theta_{Ds} D_{s,k,d}\, y_{s,k,d}\,(\gamma_t + \gamma_d) - \sum F_k^{CO2}\,\varepsilon_p \qquad (17)$$

The non-negativity constraints are described by the equations (18) - (26):

$$T_{s,k,t} \geq 0 \;\; \forall \; s\epsilon S, k\epsilon K, t\epsilon T \tag{18}$$

$$D_{s,k,d} \geq 0 \;\; \forall \; s\epsilon S, k\epsilon K, d\epsilon D \tag{19}$$

$$U_{s,k} \geq 0 \;\; \forall \; s\epsilon S, k\epsilon K \tag{20}$$

$$y_{s,k} \geq 0 \;\; \forall \; s\epsilon S, k\epsilon K \tag{21}$$

$$y_{s,k,t} \geq 0 \;\; \forall \; s\epsilon S, k\epsilon K, t\epsilon T \tag{22}$$

$$y_{s,k,d} \geq 0 \;\; \forall \; s\epsilon S, k\epsilon K, d\epsilon D \tag{23}$$

$$w_{s,k} \geq 0 \;\; \forall \; s\epsilon S, k\epsilon K \tag{24}$$

$$w_{s,k,t} \geq 0 \;\; \forall \; s\epsilon S, k\epsilon K, t\epsilon T \tag{25}$$

$$w_{s,k,d} \geq 0 \;\; \forall \; s\epsilon S, k\epsilon K, d\epsilon D \tag{26}$$

The aim of the study is to minimize the total cost of carbon integration for a certain carbon reduction target. The objective function is given in equation (27), where the total cost is the summation of carbon treatment, dehydration, inhibition, compression, transportation, and sink processing costs.

$$Min \; \sum_{s\epsilon S} \sum_{k\epsilon K} (C_{s,k}^{Treatment} + C_{s,k}^{Dehydration} + C_{s,k}^{Inhibition} + C_{s,k}^{Compression} + C_{s,k}^{Transportation} + C_{s,k}^{Sinks}) \tag{27}$$

The cost correlations for carbon treatment, compression, pumping, transportation and sink processing were adopted from Al-Mohannadi and Linke (2016) and summarized in Table (2). The carbon treatment removal parameter ε_T and the parameter γ_T were estimated to be 90% and 0.0338 ton CO_2 produced/ton CO_2 processed (Chapel et al., 1999, Gadalla et al., 2005).

The summation of the treated and dehydrated flows from source s $(D_{s,k,t})$ multiplied by the raw source carbon composition (y_s) and the carbon treatment removal parameter (ε_T) gives the carbon flow entering the dehydration unit. This flow is multiplied by the dehydration cost $(C^D_{s,k,d})$ to obtain the total dehydration cost of source s, as given in equation (29) below:

$$C^{Dehydration}_{s,k} = \sum_{s\epsilon S}\sum_{k\epsilon K}\sum_{d\epsilon D} D_{s,k,d}\, y_s\, \varepsilon_T\, C^D_s \qquad (29)$$

The total inhibition cost is equal to the total water flow multiplied by the inhibition cost. The total water flow of the untreated source s is equal to the untreated flow $(U_{s,k})$ multiplied by the raw source water composition (w_s), while the total water flow of the treated source s is the treated flow $(T_{s,k,t})$ multiplied by the overall treatment unit recovery (θ_{Ts}) and the water composition of the treated stream $(w_{s,t})$. The summation of the two terms is equal to the total inhibition cost, as shown in equation (30) below:

$$C^{Inhibition}_{s,k} = \sum_{s\epsilon S}\sum_{k\epsilon K} U_{s,k}\, w_s\, C^I_{s,k} + \sum_{s\epsilon S}\sum_{k\epsilon K}\sum_{t\epsilon T} T_{s,k,t}\, \theta_{Ts}\, w_{s,t}\, C^I_s \qquad (30)$$

After inhibitors injection, a compression is needed to account for pressure drop in pipelines and meet sinks pressure requirements. Since some of the sinks are operating at very high pressure, a phase change of carbon dioxide will take place once it reaches the critical pressure. A maximum pressure of 7.38 MPa was considered to sustain a gaseous state of CO_2, after which the stream becomes in its critical condition (McCollum and Ogden, 2006). In order to avoid two-phase flow during carbon dioxide delivery which results in an equipment damage and inefficient transmission, a pump will replace the compressor when the fluid reaches its critical point. Hence, the total compression cost is the summation of the compressors and pumps capital and operation costs. The specific power for each connection was estimated from literature using Aspen Plus simulation, based on the assumptions of known flowrates, compositions, final pressures, and pressure drop in pipelines (Al-Mohannadi and Linke, 2016). All the cost correlations were adopted from Al-Mohannadi and Linke (2016). The power carbon footprint parameter ε_p was estimated by 0.366 kg CO_2/kWh based on Karimi et al. (Karimi et al., 2012).

The carbon transportation cost is the summation of all the pipe cost parameters ($C_{s,k}^{Pipe}$), shown in equation (32), multiplied by the distance from source s to sink k ($H_{s,k}$), as described in equation (33). The pressure drop in each connection, and the distances between sources and sinks ($H_{s,k}$) were adopted from (Al-Mohannadi and Linke, 2016). The pipe diameter is calculated based on known mass flowrate, stream molecular weight, temperature, pipeline pressure drop and estimated sources outlet velocity of 20 m/s.

The pipe diameter ($D_{s,k}$) is equal to the square root of the temperature (T_s) multiplied by the total flow from source s to sink k, the gas constant ®, and ($\frac{4}{\pi}$), and divided by the flow velocity ($\upsilon_{s,k}$), stream molecular weight (m_s) and the summation of the pressure difference ($\Delta P_{s,k}$) and the pressure drop ($\Delta P_{s,k}^{pipe}$). The total flow is equal to the treated and dehydrated flow ($D_{s,k,d}$) multiplied by the treatment unit recovery (θ_{Ts}) and dehydration recovery (θ_{Ds}) added to the treated flow ($T_{s,k,t}$) multiplied by the treatment unit recovery (θ_{Ts}) plus the untreated flow ($U_{s,k}$). The pipe diameter equation is described in equation (34) below.

$$D_{s,k} = \sqrt{\frac{4}{\pi} \frac{8.314\, T_s \left(\sum_{s\epsilon S}\sum_{d\epsilon D} D_{s,k,d}\, \theta_{Ts}\theta_{Ds} + \sum_{s\epsilon S}\sum_{t\epsilon T} T_{s,k,t}\, \theta_{Ts} + \sum_{s\epsilon S} U_{s,k}\right)}{\upsilon_{s,k}\, m_s\, [\Delta P_{s,k} + \Delta P_{s,k}^{pipe}]}} \tag{34}$$

The pipe diameter is then rounded-up using equation (35), since pipelines usually have a standard size.

$$D_{s,k}^{C} = Round - Up\ (D_{s,k}) \tag{35}$$

Standard pipeline sizes are available up to a 42-inch pipe diameter. For larger flowrates, multiple pipes could be installed in parallel for delivery. An operating time of 8760 h per year was assumed for all the plants, in addition to an electricity cost of 0.02

USD/kWh, and capital recovery factor of 0.15 for capital costs annualization (Al-Mohannadi and Linke, 2016).

Table 2: Cost Correlations

Cost Element	Correlation	
Treatment Cost $\left(\frac{USD}{year}\right)$	$C_{s,k}^{Treatment} = \sum_{s\epsilon S} \sum_{k\epsilon K} \sum_{t\epsilon T} (T_{s,k,t} + D_{s,k,t})\, y_s\, C_s^T$	(28)
Compression Cost $\left(\frac{USD}{year}\right)$	$C_{s,k}^{Compression} = \sum_{s\epsilon S} \sum_{k\epsilon K} (C_{s,k}^{Compressor} + C_{s,k}^{Pump})$	(31)
Piping Cost $\left(\frac{USD}{mi}\right)$	$C_{s,k}^{pipe} = \left[95{,}230\, \left(D_{s,k}^{c}\right) + 96{,}904\right] * CRF$	(32)
Transportation Cost $\left(\frac{USD}{year}\right)$	$C_{s,k}^{Transportation} = \sum_{s\epsilon S} \sum_{k\epsilon K} C_{s,k}^{Pipe}\, H_{s,k}$	(33)
Sink Processing Cost $\left(\frac{USD}{year}\right)$	$C_{k}^{Sinks} = \sum_{k\epsilon K} F_k^{CO2}\, CR_k^{sink}$	(36)

CHAPTER V

CASE STUDY

The proposed approach is implemented on an illustrative example of Mesaieed industrial city in Qatar. All the required data about the industrial city, carbon sources and sinks can be found in (Al-Mohannadi and Linke, 2016). A map of this city is shown in Appendix B. Table (3) below represents the moisture content of the carbon sources based on (Porter et al., 2015, Zevenhoven and Kilpinen, 2001, Songolzadeh et al., 2014).

Table 3: Carbon Dioxide Sources Data

Source	CO_2 (wt. %)	H_2O (wt. %)	ρ (Kg/m^3)	C_S^T (USD/t CO_2)	C_S^D (USD/t CO_2)	CO_2 (MTPD)	H_2O (MTPD)
Ammonia-CO_2 amine unit	100	0	1.85	0	0	977	0
Steel-Iron	36.62	16.85	0.74	29	0.492	3,451	1,589
Power-gas turbine	6.6	5.6	0.82	43	0.5	9,385	7,963
Refinery-boiler	20.48	5.7	1.23	35	0.488	1,092	304

Since some of the sinks in the studied city are operating at high pressures, carbon dehydration and inhibitors injection are the two chosen methods for hydrate suppression and corrosion prevention. Although there are several technologies for dehydration that might be used, carbon dehydration using TEG is adapted in this study due to its high maturity, low cost, and high efficiency of moisture removal, noting that 200 ppm is the moisture threshold considered in this case. The dehydration cost of each source stream is estimated based on Kemper et al. (Kemper et al., 2014) and included in Table (3). Moreover, LDHIs were chosen to be injected to the streams that will not undergo a carbon dehydration, due to their relative low cost and high ability of preventing hydrate formation with very low dosage as their name indicate. The total inhibition cost is estimated to be 10 USD/ton water (ICIS, 2014). Table (4) represents the maximum allowable moisture content of all carbon sinks based on (Rushing, 2009, Brinckerhoff, 2011, Dugstad and Halseid, 2012).

Table 4: Maximum Allowable Moisture Content of CO_2 Sinks

Sinks	Max H_2O (wt. %)
Algae	5.6
Greenhouses	0.03
Methanol	0.05
Urea	0.05
EOR	0.03
Saline Storage	0.03

A. Results and Discussion

The Mixed Integer Non-Linear Program (MINLP) formulated in the previous section has been implemented using “What'sBest 15.0” Lindo Global solver for MS-Excel 2016 via a laptop with Intel Core i5 Duo processor, 8 GB RAM and a 64-bit operating System.

In order to investigate the effect of carbon footprint reduction goals on the flows and types of connections, the optimization problem was solved for a set of carbon reduction goals ranging from 5% to 30%, since many countries are reducing their CO_2 emissions by 30%. The minimum total annual cost of the carbon integration networks ranged from -8.74 million USD, i.e. profitable operation, to 91.97 million USD. Figures (4) - (7) show the identified optimal integration networks.

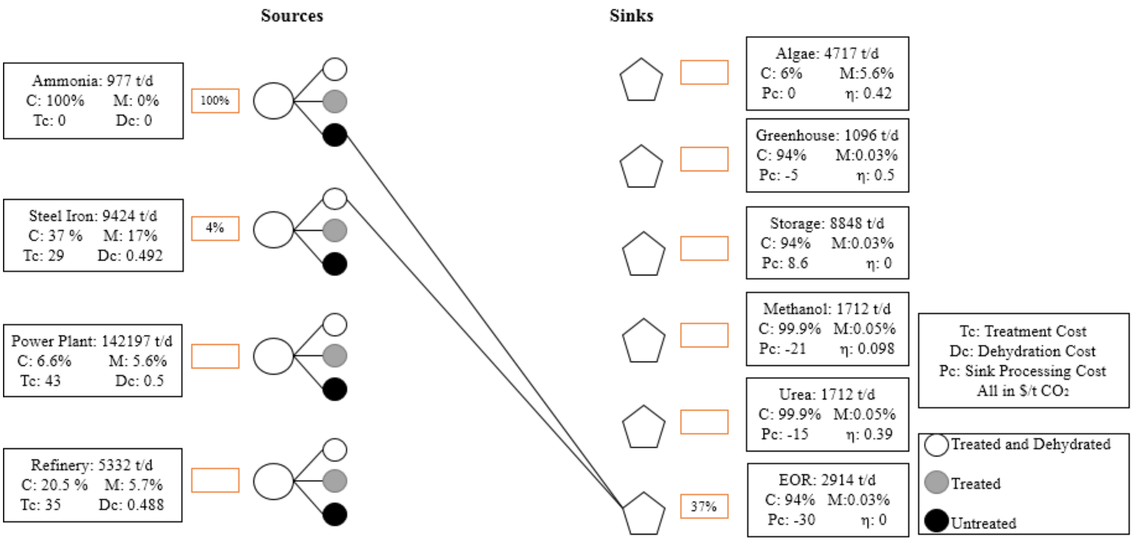

Figure 4: Carbon Integration Network for 5% Net Capture Reduction Target

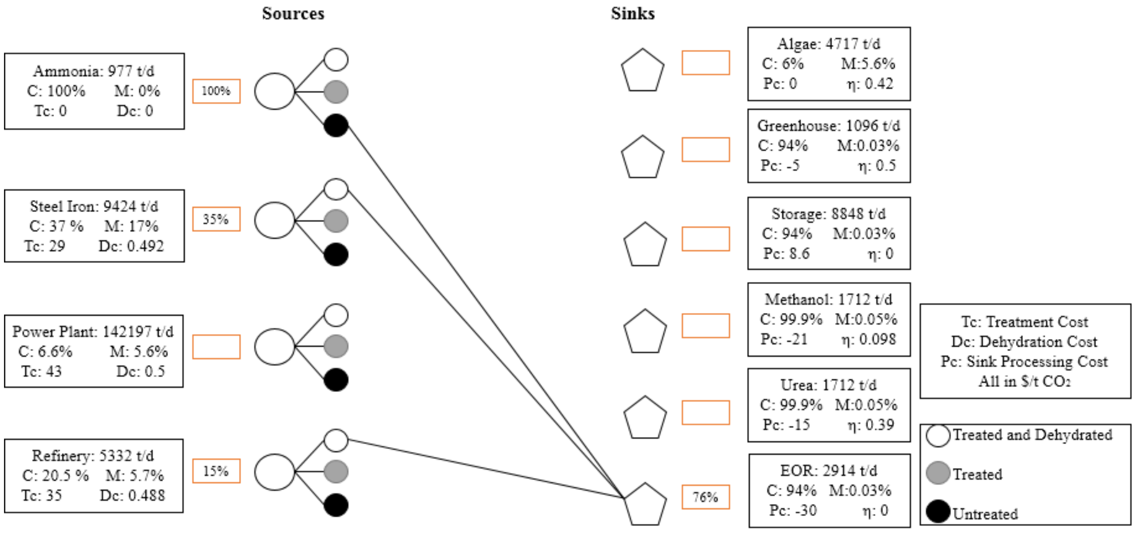

Figure 5: Carbon Integration Network for 10% Net Capture Reduction Target

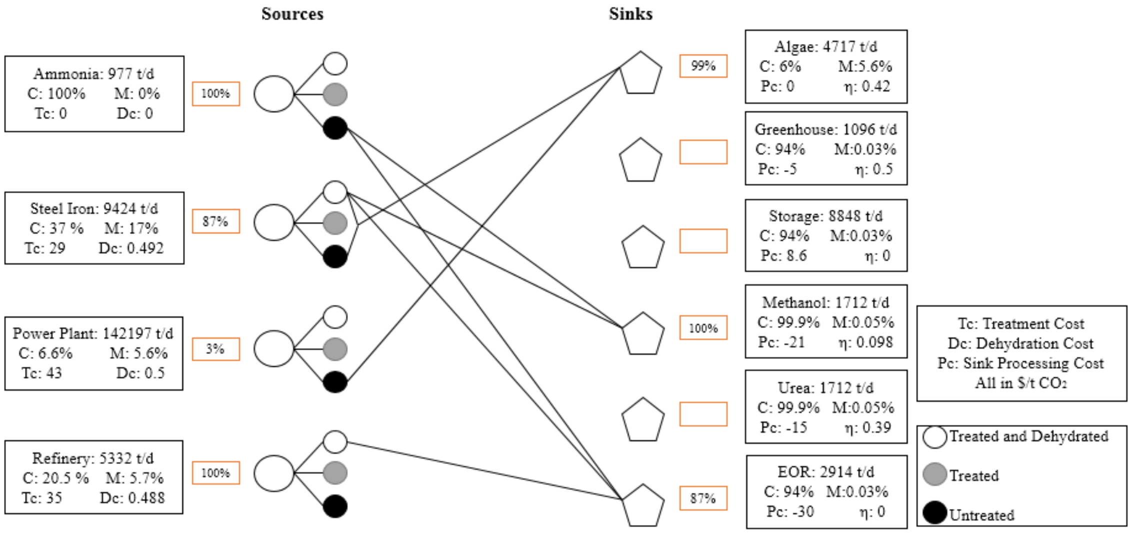

Figure 6: Carbon Integration Network for 20% Net Capture Reduction Target

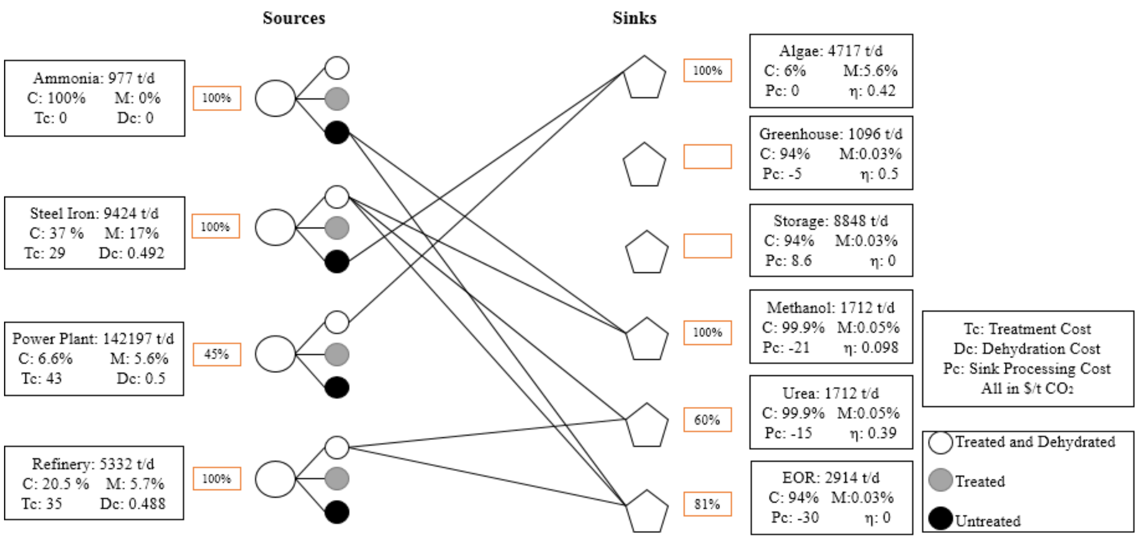

Figure 7: Carbon Integration Network for 30% Net Capture Reduction Target

For the case of 5% net carbon reduction target (Fig. 4), a profitable carbon integration network has been obtained. The first selected source, in this case, is the carbon dioxide from the ammonia plant which is the purest carbon source. Therefore, no carbon separation or dehydration are needed due to the high purity of this source. The steel iron mill source, which is the second purest source was also selected to be used in treated and dehydrated condition. On the other hand, enhanced oil recovery (EOR), which is the sink with the highest revenue, is the only selected sink. The total revenue of the network outweighs the compression and delivery costs, resulting in a profitable allocation with a net profit of 8.74 million USD per year.

When the net carbon reduction target is increased to 10% (Fig. 5), EOR remains the only selected sink. However, one additional source, the refinery plant, is involved in this case, which is the third purest source. Since this source contain significant amounts of moisture and other contaminants, treated and dehydrated carbon streams from these sources are mixed with the untreated stream from the ammonia plant source. Hence, additional costs are incurred due to the treatment and dehydration of the carbon streams, but the allocation remains profitable with a slight net profit decrease to 5.32 million USD per year.

The network becomes more complex with all sources being involved and 3 active sinks, when the net carbon reduction target is increased to 20% (Fig. 6). The enhanced oil recovery sink receives its carbon dioxide flows from the same sources of the previous case. On the other hand, algae growth is the sink with the highest allowable moisture content. Therefore, it is the second sink to be involved with a feed that includes a mixture of treated and dehydrated and untreated carbon dioxide from steel iron mill, in addition to untreated CO_2 from the power plant. Moreover, methanol plant has the second highest revenue and efficiency. Hence, it is the third active sink with a carbon purity requirement of 99.9%. Consequently, a mixture of carbon from ammonia plant and treated and dehydrated carbon from steel iron mill is delivered to this sink. In this case, a total inhibition cost of 955 thousand USD per year is added due to the use of inhibitors in the untreated carbon streams from the steel iron mill and power plant. The overall allocation is no longer profitable, and the cost of the optimal carbon integration network increases to 14 million USD per year.

When the net carbon reduction target is increased further to 30% (Fig. 7), the urea plant becomes an active sink beside the algae, methanol plant and EOR. At this point, the mixing of carbon from the steel source that is observed in the previous case disappeared. This can be related to the urea sink requirement of carbon with very high purity. Therefore, its need is fulfilled by treated and dehydrated carbon from the steel iron mill and refinery plant, whereas a higher flowrate of untreated carbon mixed with treated and dehydrated carbon from the power plant is delivered to the algae sink which can accommodate high amount of moisture compared to the other sinks. The source streams allocated to the methanol plant come from the ammonia plant and treated and dehydrated carbon from the steel iron mill. On the other hand, the carbon dioxide transported to the EOR sink comes from the same sources of the previous case. This network results in a minimum annual cost of 91.97 million USD per year. The dramatic increase in the carbon integration cost, which occurred when the net carbon reduction target is increased from 20% to 30%, is due to the high exploitation of the power plant source. This source is characterized by having the lowest purity and highest treatment cost. Therefore, large amounts of flue gas from this source should be treated and dehydrated in order to provide a certain carbon dioxide flowrate. Consequently, the treatment cost increases from 45 million USD per year at 20% carbon reduction to 123 million USD per year at 30% reduction, resulting in a significant increase in the total cost of carbon integration.

The highest carbon reduction target that could be achieved was found to be 32.1%. At this point, all the connections remain the same as in the previous case, except for the algae sink which now receives its carbon requirement from a mixture of treated and dehydrated and untreated carbon from the power plant. Moreover, the flowrates of some connections are changed, resulting in removing over 6570 MTD of net carbon dioxide at a minimum total cost of 113 million USD per year. Figure (8) summarizes the specific costs of carbon integration networks as a function of the net carbon reduction target in the industrial park.

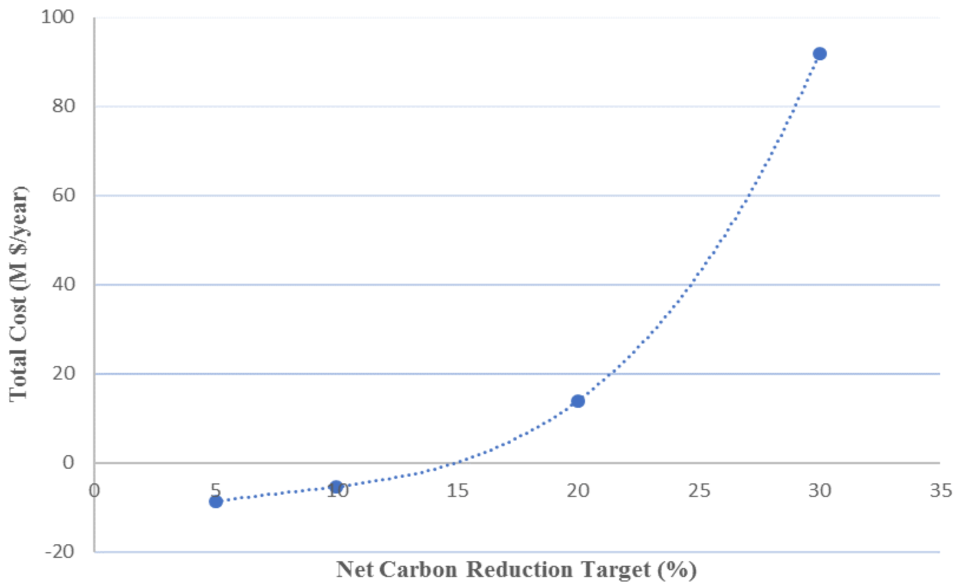

Figure 8: Carbon Integration Network Cost per Net Carbon Reduction Target

The emissions associated with treatment and dehydration recovery inefficiencies, power supply, and sinks processing efficiencies are accounted for in the calculation of the specific costs. It was found that carbon integration is profitable up to a net reduction target of around 15%, and the cost per ton of carbon dioxide is relatively inexpensive, even after that point, compared to other carbon tax values (World Bank, 2016). It is also worth to note that carbon dehydration and hydrate inhibition costs consist a small fraction of the total cost, as they together account for a value that does not exceed 3% of the total carbon integration cost. Figures (9) – (11) represent the cost of each process in the optimal carbon networks at three carbon dioxide net reduction targets in terms of treatment, dehydration, inhibition, compression, transportation, and sink processing costs.

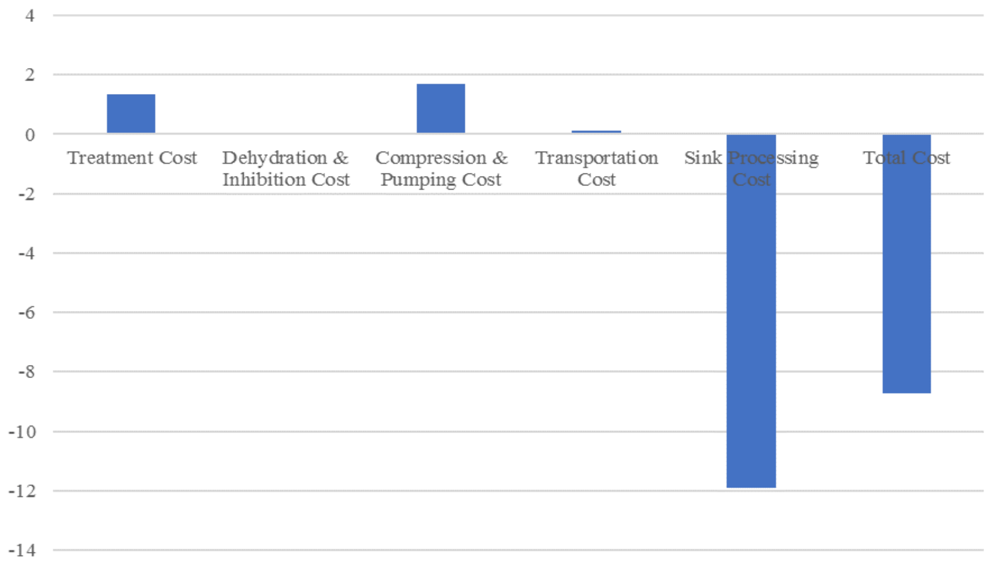

Figure 9: Processes Specific Costs for 5% Net Carbon Reduction Target

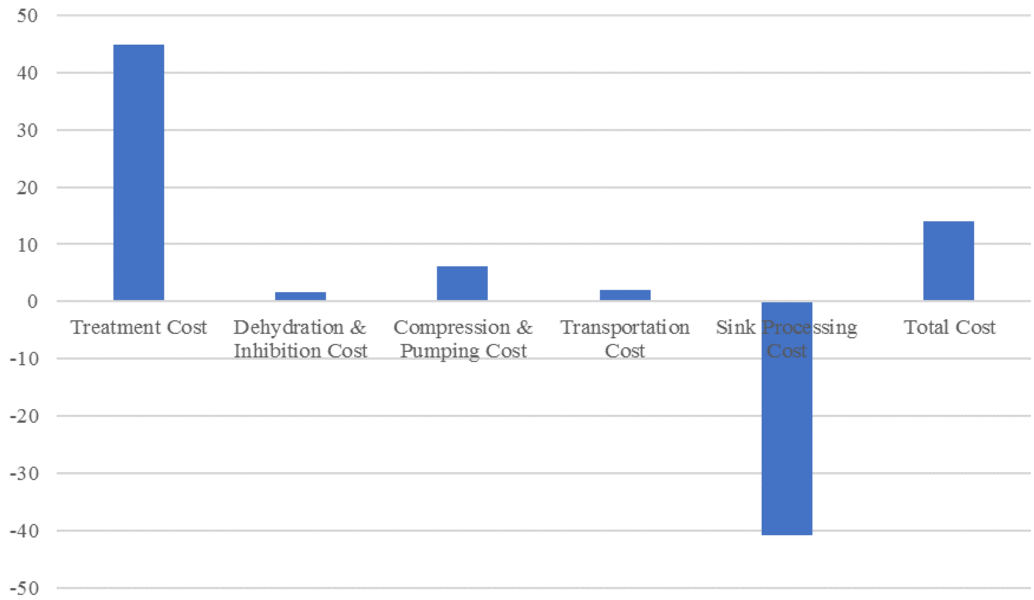

Figure 10: Processes Specific Costs for 20% Net Carbon Reduction Target

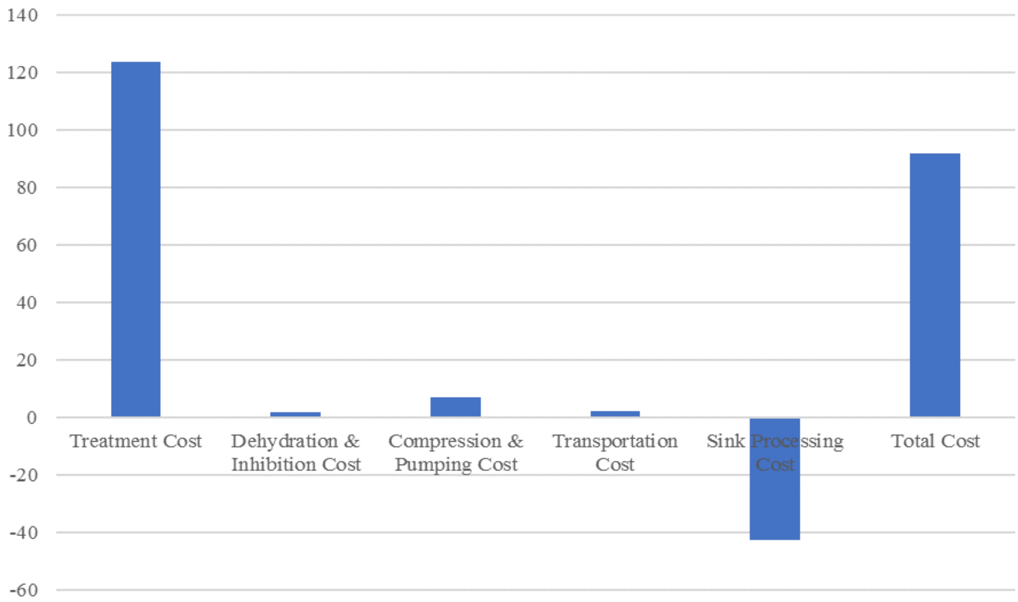

Figure 11: Processes Specific Costs for 30% Net Carbon Reduction Target

Figure (12) below shows a comparison between the total costs associated with different net carbon reduction targets for the work done by (Al-Mohannadi and Linke, 2016) and this work. The highest reduction target that was achieved by their work was 50% which is greater than the highest target of 32.1% in this work. The main reason is the constraints related to the presence of moisture that is considered in this work which resulted in a decrease in the highest achievable reduction target. Moreover, it is clear that the total costs of the networks synthesized in this work are always higher than those of Al-Mohannadi and Linke’s work, and this is due to the dehydration and inhibition costs that are added in this work. In addition, there is an increase in the treatment cost, since the consideration of moisture leads to the release of higher amounts of carbon from the carbon capture and dehydration units to the atmosphere. Therefore, larger flowrates of carbon are required in order to achieve the desired reduction targets.

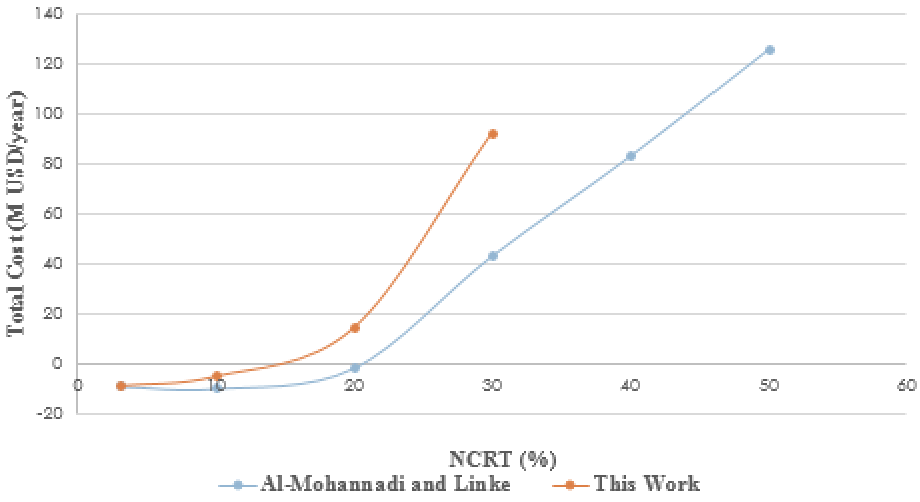

Figure 12 : Comparison of Carbon Integration Network Costs

After comparing the obtained results for different net carbon reduction targets, there are several observations that raise some questions about. For instance, in all the studied cases, the two preferred options for carbon allocation are the “untreated” and “treated and dehydrated” options, while the “treated” option is not considered in any case. The preference of the “treated and dehydrated” option is mainly due to the inhibition cost (10 USD/ton of water) associated with this option, due to the presence of significant amount of moisture after carbon treatment, which is relatively high compared to the dehydration cost (~ 0.5 USD/ton of CO_2). Another observation is that greenhouse sink is not chosen by any network, although it consists a source of revenue, same as the saline storage sink which is not used at all, even though it has a very high efficiency. Therefore, the next section represents a sensitivity analysis in which the three mentioned observations will be analyzed in order to investigate the reasons behind their occurrence.

B. Sensitivity Analysis

The optimal solution in each of the five studied cases depends on several parameters including treatment and dehydration costs, distances between sources and sinks, units’ efficiencies and many others. Therefore, any change in one of these parameters will lead to a different optimal network, hence, a different total cost of carbon dioxide allocation. A sensitivity analysis helps in interpreting the obtained solutions and understanding how the decision variables will vary, when one or more of the coefficients in the objective function is modified.

The first observation that will be investigated is the absence of the “treated” carbon option in all the studied cases. Therefore, the aim here is to find the case in which the “treated” carbon option will be considered in a specific network. As previously mentioned, since the inhibition cost is relatively high compared to the dehydration cost, the “treated and dehydrated” carbon option is always preferred over the “treated” carbon option. Consequently, decreasing the inhibition cost is one way to make the “treated” option appear. However, this method does not work in any of the studied cases for a main reason that is carbon dehydration is already very cheap. In other words, even if the inhibition cost is reduced below the dehydration cost, the system will still prefer the “treated and dehydrated” option which provides it with highly pure carbon dioxide streams, especially that some sinks, such as methanol and urea plants, require a 99.9% pure carbon. On the other hand, when the dehydration cost increases above the inhibition cost, the “treated” carbon option starts appearing. It was found that this option appears, for the first time, when the dehydration cost increases to 28 USD/ton of CO_2 at a reduction target of 20%. This value decreases to 11 USD/ton of CO_2, when the reduction target becomes 30%. Hence, as the net carbon reduction target increases, higher carbon flowrate is required from the sources, resulting in a consideration of the “treated” option even at a small difference between the dehydration and inhibition costs. Figure (13) illustrates the modifications that occurred to the carbon integration network with a 30% reduction target, when the dehydration cost is increased to 11 USD/ton of CO_2. In this case, around 311 MTD of “treated” carbon from the power plant is allocated to the algae sink. Moreover, the total annual cost of this network is affected by the increase in the dehydration cost, and it becomes around 120 million USD per year.

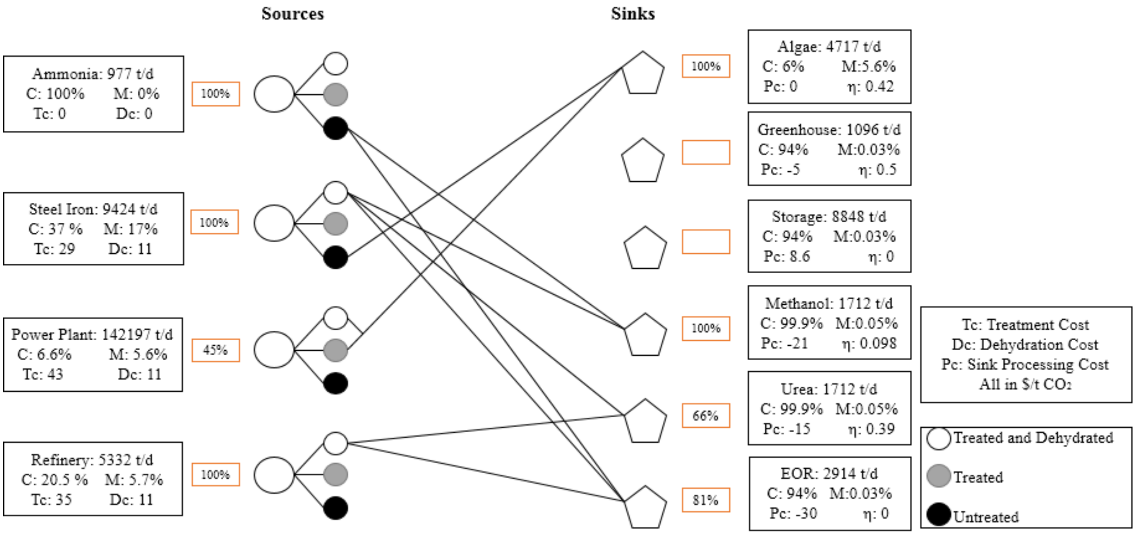

Figure 13: Carbon Integration Network for 30% net capture with modification of dehydration cost

The dehydration unit recovery is another parameter that can affect the optimal solution in a way that "treated" carbon option will be considered in the network, since as the dehydration unit recovery decreases, the "treated" carbon option gains preference over the "treated and dehydrated" option. It was found that when the dehydration unit recovery decreases to 54% at a reduction target of 10%, the "treated" carbon option starts to appear in the network. When the reduction target is increased to 20%, the "treated" option appears, for the first time, at a dehydration unit recovery of 68%, while it does not appear at all, when the reduction target is further increased to 30%. This behavior was expected, since as the net reduction target increases, the minimum required recovery increases in order to provide the needed amount of carbon dioxide. In the case of 20% reduction target with 68% dehydration unit recovery, around 14 MTD of “treated” carbon from the steel iron mill is allocated to the algae sink, resulting in an integration network with a total annual cost of 90.5 million USD per year. It is interesting to note that, in all the cases that were modified for the sake of making the “treated” option being considered, the first sink that was chosen by the system to accept the carbon from the “treated” option is the algae sink, and this is due to the fact that this sink has the highest allowable moisture content of 5.6%, which explains its capability of accepting carbon streams with significant amount of moisture.

The second observation to be investigated is the absence of saline storage sink from all the optimal networks. It is obvious that the reason behind this is that the processing cost of this sink is very high (8.6 USD/ton of CO_2) compared to all other sinks which are sources of revenue for the system. Therefore, it was found that by decreasing the processing cost to -31 USD/ton of CO_2, this sink will get a high potential of being used in the carbon integration networks for all reduction targets. It is worth to note that saline storage sink has an advantage of having a 100% efficiency, meaning that no carbon losses would take place. However, its maximum allowable moisture content is 300 ppm, which is the lowest between all the other sinks. Hence, it was found that by increasing this value to 450 ppm without changing the initial processing cost (8.6 USD), the saline storage sink will be activated at a net carbon reduction target of 30%. The modified network is represented in Figure (14), where 664 MTD of carbon dioxide are allocated to the storage sink, resulting in a total carbon integration annual cost of 87.8 million USD per year.

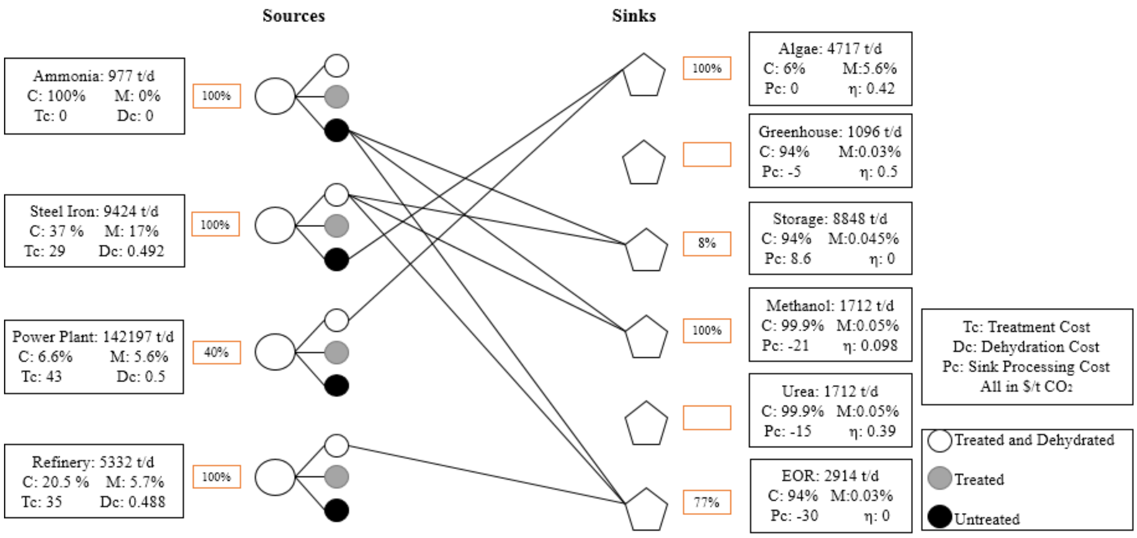

Figure 14: Carbon Integration Network for 30% net capture with modification of saline storage sink parameters

Although it is a source of revenue, greenhouse sink is not considered in any of the carbon networks associated with different reduction targets. The main reason behind this is the long distances between this sink and all the sources which increase the delivery cost, since it is located outside the industrial park. Assuming shorter distances separating the sources from greenhouse sink does not activate this sink in any of the studied cases. Thus, there are other parameters that prevent this sink from being used. These parameters are the low sink efficiency of 50% and maximum allowable moisture content of 300 ppm. Hence, the greenhouse sink appears in the carbon integration network, for the first time, when its efficiency is increased to 100% and its maximum allowable moisture content is increased to 400 ppm at a reduction target of 30%. Figure (15) shows the modified network in which 949 MTD of carbon dioxide are allocated to the greenhouse sink, resulting in a total annual cost of 85.3 million USD per year.

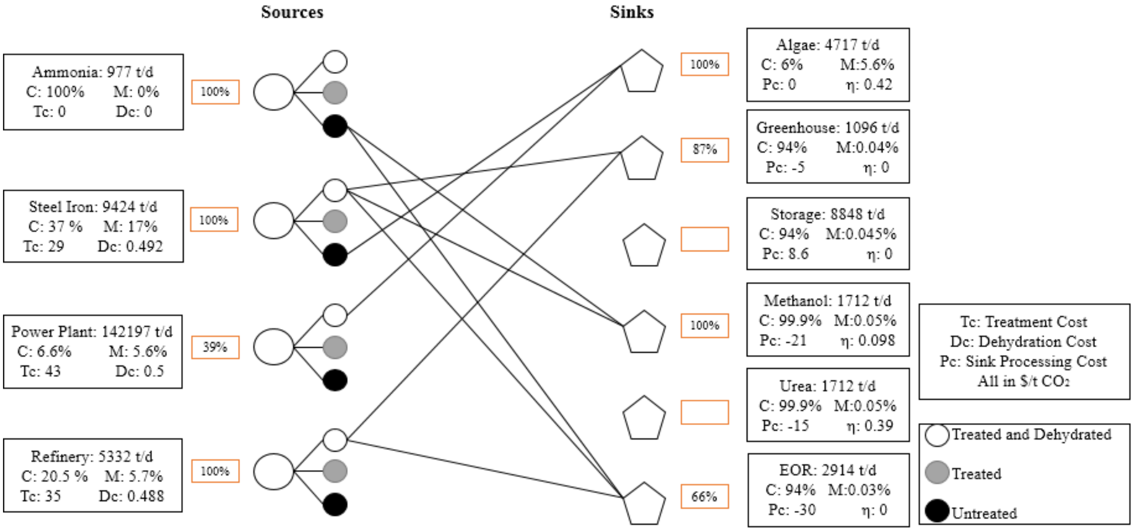

Figure 15: Carbon Integration Network for 30% net capture with modification of greenhouse sink parameters

Figures (16)-(18) represent the impact of dehydration cost, sink efficiency, and maximum allowable moisture content on the total carbon reduction cost, respectively. Figure (16) shows that the total reduction cost increases linearly with the dehydration cost. Increasing the dehydration cost from 0.5 to 20 USD/ton CO_2 have resulted in a 54% increase in the total reduction cost. The main reason behind this increase is that the dehydration cost is highly related to all carbon sources, especially for high net carbon reduction targets. In fact, when a higher carbon reduction target is required, more "treated and dehydrated" carbon flowrates are needed, leading to a higher total carbon reduction cost.

The effects of sinks maximum allowable moisture contents and efficiencies on the total reduction cost are shown in Figures (17) and (18), respectively. The total reduction cost is more related to sink processing cost than two studied parameters. In other words, the high maximum allowable moisture content and sink efficiency are two important parameter that affect the decision of activating a specific sink. However, once a sink is being activated due to its high allowable moisture content or efficiency, its processing cost will determine whether the total reduction cost will increase or decrease. For instance, the saline storage sink has a 100% efficiency and a total processing cost of 8.6 USD/ton CO_2, meaning that higher processing cost will result from a higher carbon flowrate allocated to this sink. However, the greenhouse sink provides a revenue of 5 USD/ton CO_2 allocated. Therefore, when its efficiency was increased to 100%, its revenue increases resulting in a decrease of 8% in the total reduction cost.

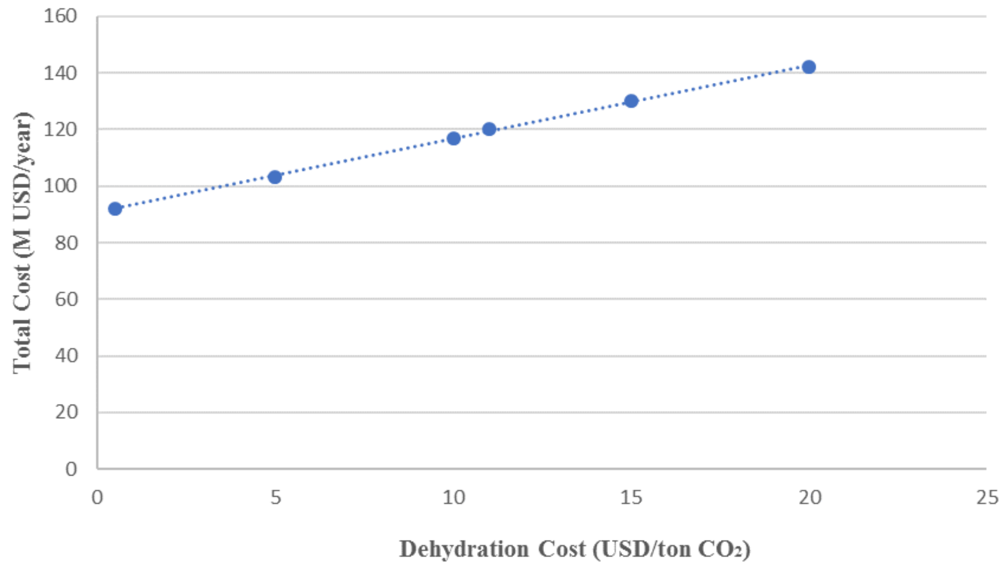

Figure 16: Carbon Integration Network Cost vs Dehydration Cost for 30% NCRT

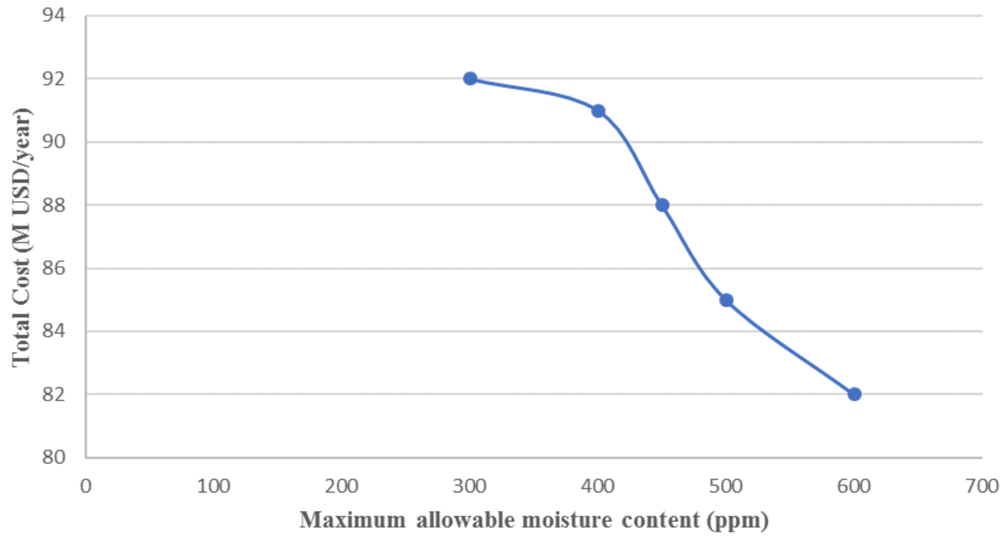

Figure 17: Carbon Integration Network Cost vs Storage maximum allowable moisture content for 30% NCRT

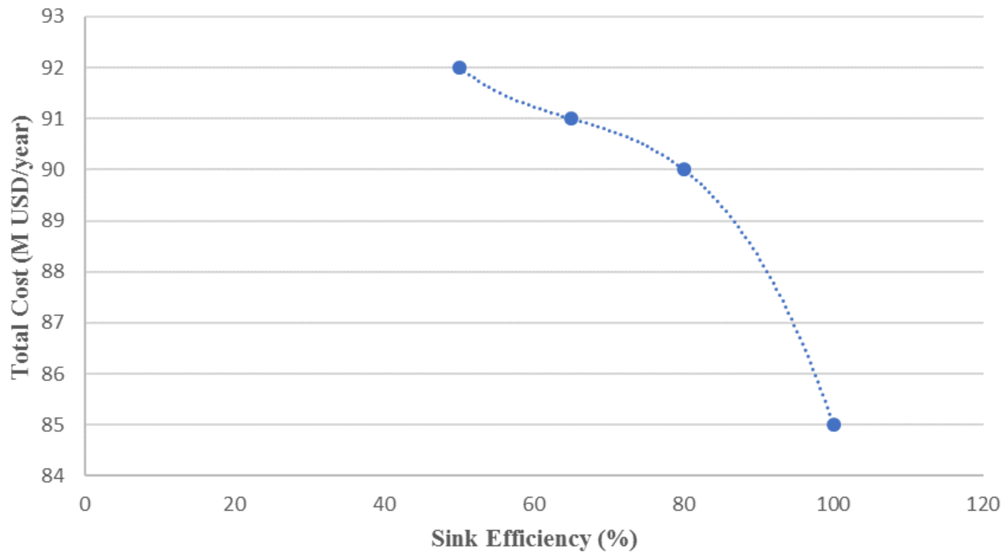

Figure 18: Carbon Integration Network Cost vs Greenhouse sink Efficiency for 30% NCRT

CHAPTER VI

CONCLUSION

The conducted study presented an approach for carbon integration networks by proposing several options for transferring the captured carbon dioxide to the potential sinks. Regardless of the absence of standards for drying requirements in CO_2 pipelines, this study considered the maximum allowable moisture content of carbon sinks, in addition to suggesting different methods for hydrate suppression and corrosion prevention in pipelines. The importance of this approach lies in its ability of being applied in any industrial city aiming at reducing its carbon footprint under the supervision of policy makers. The presented case study illustrated the effectiveness of the proposed approach by exploring the costs and designs of the different stages of the overall process. A sensitivity analysis was also performed in order to investigate the effect of several parameters on the resulted carbon networks. The deployment of multiple dehydration technologies options can be investigated in future work, while the use of renewable energy for carbon capture and dehydration units is recommended for achieving high reduction targets with lower costs.

APPENDIX I

CASE STUDY DETAILED RESULTS

This section represents the detailed results of each of the five cases performed in the case study. All the flowrates are given in MTPD, while the costs are expressed in USD/year.

U, T, and D are the abbreviations used for the untreated option, treated option, and treated and dehydrated option, respectively.

A1. CO_2 Exchange Streams

Table 5: Carbon allocation for 5% NCRT

Exchange	Algae	Greenhouse	Storage	Methanol	Urea	EOR
Ammonia U	0	0	0	0	0	977
Steel U	0	0	0	0	0	0
Power U	0	0	0	0	0	0
Refinery U	0	0	0	0	0	0
Ammonia T	0	0	0	0	0	0
Steel T	0	0	0	0	0	0
Power T	0	0	0	0	0	0
Refinery T	0	0	0	0	0	0
Ammonia D	0	0	0	0	0	0
Steel D	0	0	0	0	0	338.35
Power D	0	0	0	0	0	0
Refinery D	0	0	0	0	0	0

Table 6: Carbon allocation for 10% NCRT

Exchange	Algae	Greenhouse	Storage	Methanol	Urea	EOR

Ammonia U	0	0	0	0	0	977
Steel U	0	0	0	0	0	0
Power U	0	0	0	0	0	0
Refinery U	0	0	0	0	0	0
Ammonia T	0	0	0	0	0	0
Steel T	0	0	0	0	0	0
Power T	0	0	0	0	0	0
Refinery T	0	0	0	0	0	0
Ammonia D	0	0	0	0	0	0
Steel D	0	0	0	0	0	3323.4
Power D	0	0	0	0	0	0
Refinery D	0	0	0	0	0	810.7

Table 7: Carbon allocation for 20% NCRT

Exchange	Algae	Greenhouse	Storage	Methanol	Urea	EOR
Ammonia U	0	0	0	188.8	0	788.2
Steel U	179.74	0	0	0	0	0
Power U	4130.69	0	0	0	0	0
Refinery U	0	0	0	0	0	0
Ammonia T	0	0	0	0	0	0
Steel T	0	0	0	0	0	0
Power T	0	0	0	0	0	0
Refinery T	0	0	0	0	0	0
Ammonia D	0	0	0	0	0	0
Steel D	1106.09	0	0	4618.15	0	2281.8
Power D	0	0	0	0	0	0
Refinery D	0	0	0	0	0	5332.03

Table 8: Carbon allocation for 30% NCRT

Exchange	Algae	Greenhouse	Storage	Methanol	Urea	EOR
Ammonia U	0	0	0	188.8	0	788.2
Steel U	946.54	0	0	0	0	0
Power U	0	0	0	0	0	0
Refinery U	0	0	0	0	0	0
Ammonia T	0	0	0	0	0	0

Steel T	0	0	0	0	0	0
Power T	0	0	0	0	0	0
Refinery T	0	0	0	0	0	0
Ammonia D	0	0	0	0	0	0
Steel D	0	0	0	4618.15	1489.23	2369.9
Power D	63405	0	0	0	0	0
Refinery D	0	0	0	0	1031.86	4300.17

Table 9: Carbon allocation for 32.1% NCRT

Exchange	Algae	Greenhouse	Storage	Methanol	Urea	EOR
Ammonia U	0	0	0	188.8	0	788.2
Steel U	0	0	0	0	0	0
Power U	1.65	0	0	0	0	0
Refinery U	0	0	0	0	0	0
Ammonia T	0	0	0	0	0	0
Steel T	0	0	0	0	0	0
Power T	0	0	0	0	0	0
Refinery T	0	0	0	0	0	0
Ammonia D	0	0	0	0	0	0
Steel D	0	0	0	4618.15	2382.9	2422.76
Power D	79295.7	0	0	0	0	0
Refinery D	0	0	0	0	1651.07	3680.96

A2. Detailed Costs for 5% NCRT

For a net carbon reduction target of 5%, the total flowrate of captured CO_2 is 1023.2 MTPD. In this case, there is no inhibition cost, since the two sources used are the pure ammonia source and the treated and dehydrated steel source.

Table 10: Detailed Costs for 5% NCRT

Treatment Cost						
Exchange	Algae	Greenhouse	Storage	Methanol	Urea	EOR

Ammonia	0	0	0	0	0	0
Steel	0	0	0	0	0	1339478
Power	0	0	0	0	0	0
Refinery	0	0	0	0	0	0
Dehydration Cost						
Exchange	Algae	Greenhouse	Storage	Methanol	Urea	EOR
Ammonia	0	0	0	0	0	0
Steel	0	0	0	0	0	20033.17
Power	0	0	0	0	0	0
Refinery	0	0	0	0	0	0
Compression Cost						
Exchange	Algae	Greenhouse	Storage	Methanol	Urea	EOR
Ammonia	0	0	0	0	0	882294.2
Steel	0	0	0	0	0	115706.7
Power	0	0	0	0	0	0
Refinery	0	0	0	0	0	0
Pumping Cost						
Exchange	Algae	Greenhouse	Storage	Methanol	Urea	EOR
Ammonia	0	0	0	0	0	621384.04
Steel	0	0	0	0	0	81351.24
Power	0	0	0	0	0	0
Refinery	0	0	0	0	0	0
Transportation Cost						
Exchange	Algae	Greenhouse	Storage	Methanol	Urea	EOR
Ammonia	0	0	0	0	0	69322.98
Steel	0	0	0	0	0	51044.62
Power	0	0	0	0	0	0
Refinery	0	0	0	0	0	0
Processing Cost						
Exchange	Algae	Greenhouse	Storage	Methanol	Urea	EOR
Ammonia	0	0	0	0	0	-1.1E+07
Steel	0	0	0	0	0	0
Power	0	0	0	0	0	0
Refinery	0	0	0	0	0	0

A3. Detailed Costs for 10% NCRT

For a net carbon reduction target of 10%, the total flowrate of captured CO_2 is 2046.4 MTPD. Similarly, there are treatment and dehydration costs, since the treated and dehydrated option is used, but also there is no inhibition cost because the only active source that is being used as untreated carbon is the ammonia plant.

Table 11: Detailed Costs for 10% NCRT

Treatment Cost						
Exchange	Algae	Greenhouse	Storage	Methanol	Urea	EOR
Ammonia	0	0	0	0	0	0
Steel	0	0	0	0	0	13156640
Power	0	0	0	0	0	0
Refinery	0	0	0	0	0	2011529
Dehydration Cost						
Exchange	Algae	Greenhouse	Storage	Methanol	Urea	EOR
Ammonia	0	0	0	0	0	0
Steel	0	0	0	0	0	196770.1
Power	0	0	0	0	0	0
Refinery	0	0	0	0	0	26619.98
Compression Cost						
Exchange	Algae	Greenhouse	Storage	Methanol	Urea	EOR
Ammonia	0	0	0	0	0	882294.2
Steel	0	0	0	0	0	983913.3
Power	0	0	0	0	0	0
Refinery	0	0	0	0	0	150191.9
Pumping Cost						
Exchange	Algae	Greenhouse	Storage	Methanol	Urea	EOR
Ammonia	0	0	0	0	0	621384
Steel	0	0	0	0	0	696767.1
Power	0	0	0	0	0	0
Refinery	0	0	0	0	0	103672.5
Transportation Cost						
Exchange	Algae	Greenhouse	Storage	Methanol	Urea	EOR
Ammonia	0	0	0	0	0	69322.98
Steel	0	0	0	0	0	84876.21
Power	0	0	0	0	0	0
Refinery	0	0	0	0	0	21914.45
Processing Cost						
Exchange	Algae	Greenhouse	Storage	Methanol	Urea	EOR
Ammonia	0	0	0	0	0	-1.1E+07
Steel	0	0	0	0	0	-1.2E+07
Power	0	0	0	0	0	0

Refinery	0	0	0	0	0	-1636245

A4. Detailed Costs for 20% NCRT

For a net carbon reduction target of 20%, the total flowrate of captured CO_2 is 4092.8 MTPD.

Table 12: Detailed Costs for 20% NCRT

Treatment Cost						
Exchange	Algae	Greenhouse	Storage	Methanol	Urea	EOR
Ammonia	0	0	0	0	0	0
Steel	4378765	0	0	18282276	0	9033155
Power	0	0	0	0	0	0
Refinery	0	0	0	0	0	13229921
Dehydration Cost						
Exchange	Algae	Greenhouse	Storage	Methanol	Urea	EOR
Ammonia	0	0	0	0	0	0
Steel	65488.6	0	0	273428.8	0	135099.4
Power	0	0	0	0	0	0
Refinery	0	0	0	0	0	175080.9
Inhibition Cost						
Exchange	Algae	Greenhouse	Storage	Methanol	Urea	EOR
Ammonia	0	0	0	0	0	0
Steel	110546	0	0	0	0	0
Power	844312	0	0	0	0	0
Refinery	0	0	0	0	0	0
Compression Cost						
Exchange	Algae	Greenhouse	Storage	Methanol	Urea	EOR
Ammonia	0	0	0	186979.6	0	719798.6
Steel	65351.4	0	0	1344976	0	688837.9
Power	540967	0	0	0	0	
Refinery	0	0	0	0	0	887548.2
Pumping Cost						
Exchange	Algae	Greenhouse	Storage	Methanol	Urea	EOR
Ammonia	0	0	0	20353.9	0	503338

Steel	0	0	0	91393	0	481681
Power	0	0	0	0	0	0
Refinery	0	0	0	0	0	623300
Transportation Cost						
Exchange	Algae	Greenhouse	Storage	Methanol	Urea	EOR
Ammonia	0	0	0	40354.65	0	41690.9
Steel	458643	0	0	82654.32	0	51044.62
Power	1349709	0	0	0	0	0
Refinery	0	0	0	0	0	36439
Processing Cost						
Exchange	Algae	Greenhouse	Storage	Methanol	Urea	EOR
Ammonia	0	0	0	-1447103	0	-8630861
Steel	0	0	0	-1.2E+07	0	-8234787
Power	0	0	0	0	0	0
Refinery	0	0	0	0	0	-1.1E+07

A5. Detailed Costs for 30% NCRT

For a net carbon reduction target of 30%, the total flowrate of captured CO_2 is 6139.2 MTPD.

Table 13: Detailed Costs for 30% NCRT

Treatment Cost						
Exchange	Algae	Greenhouse	Storage	Methanol	Urea	EOR
Ammonia	0	0	0	0	0	0
Steel	0	0	0	18282276	5895525	9381915
Power	7.7E+07	0	0	0	0	0
Refinery	0	0	0	0	2560266	10669655
Dehydration Cost						
Exchange	Algae	Greenhouse	Storage	Methanol	Urea	EOR
Ammonia	0	0	0	0	0	0
Steel	0	0	0	273428.8	88173.19	140315.5
Power	687917	0	0	0	0	0
Refinery	0	0	0	0	33881.8	141199
Inhibition Cost						
Exchange	Algae	Greenhouse	Storage	Methanol	Urea	EOR

Ammonia	0	0	0	0	0	0
Steel	582144	0	0	0	0	0
Power	0	0	0	0	0	0
Refinery	0	0	0	0	0	0
Compression Cost						
Exchange	Algae	Greenhouse	Storage	Methanol	Urea	EOR
Ammonia	0	0	0	186979.6	0	719798.6
Steel	109523	0	0	1344976	460075.1	714003.9
Power	496221	0	0	0	0	0
Refinery	0	0	0	0	188340.3	723838.9
Pumping Cost						
Exchange	Algae	Greenhouse	Storage	Methanol	Urea	EOR
Ammonia	0	0	0	20354	0	503338
Steel	0	0	0	91393	276158	499873
Power	0	0	0	0	0	0
Refinery	0	0	0	0	112797	504710
Transportation Cost						
Exchange	Algae	Greenhouse	Storage	Methanol	Urea	EOR
Ammonia	0	0	0	40354.65	0	41690.9
Steel	568640	0	0	82654.32	50777.38	51044.62
Power	1300644	0	0	0	0	0
Refinery	0	0	0	0	17638.46	21914.45
Processing Cost						
Exchange	Algae	Greenhouse	Storage	Methanol	Urea	EOR
Ammonia	0	0	0	-1447103	0	-8630861
Steel	0	0	0	-1.2E+07	-2687234	-8552723
Power	0	0	0	0	0	0
Refinery	0	0	0	0	-1041303	-8679054

A6. Detailed Costs for 32.1% NCRT

For a net carbon reduction target of 32.1%, the total flowrate of captured CO_2 is 6570 MTPD.

Table 14: Detailed Costs for 32.1% NCRT

Treatment Cost						
Exchange	Algae	Greenhouse	Storage	Methanol	Urea	EOR

Ammonia	0	0	0	0	0	0
Steel	0	0	0	18282276	9433377	9591203
Power	9.6E+07	0	0	0	0	0
Refinery	0	0	0	0	4096659	9133262
Dehydration Cost						
Exchange	Algae	Greenhouse	Storage	Methanol	Urea	EOR
Ammonia	0	0	0	0	0	0
Steel	0	0	0	273428.8	141085.1	143445.6
Power	860324	0	0	0	0	0
Refinery	0	0	0	0	54213.97	120866.9
Inhibition Cost						
Exchange	Algae	Greenhouse	Storage	Methanol	Urea	EOR
Ammonia	0	0	0	0	0	0
Steel	0	0	0	0	0	0
Power	338.138	0	0	0	0	0
Refinery	0	0	0	0	0	0
Compression Cost						
Exchange	Algae	Greenhouse	Storage	Methanol	Urea	EOR
Ammonia	0	0	0	186979.6	0	719798.6
Steel	0	0	0	1344976	717713.6	729084.9
Power	613306	0	0	0	0	0
Refinery	0	0	0	0	293043.4	624739.8
Pumping Cost						
Exchange	Algae	Greenhouse	Storage	Methanol	Urea	EOR
Ammonia	0	0	0	20354	0	503338
Steel	0	0	0	91393	435577	510789
Power	0	0	0	0	0	0
Refinery	0	0	0	0	174185	433546
Transportation Cost						
Exchange	Algae	Greenhouse	Storage	Methanol	Urea	EOR
Ammonia	0	0	0	40354.65	0	41690.9
Steel	0	0	0	82654.32	50777.38	51044.62
Power	1447838	0	0	0	0	0
Refinery	0	0	0	0	17638.46	21914.45
Processing Cost						
Exchange	Algae	Greenhouse	Storage	Methanol	Urea	EOR
Ammonia	0	0	0	-1447103	0	-8630861
Steel	0	0	0	-1.2E+07	-4299819	-8743514
Power	0	0	0	0	0	0
Refinery	0	0	0	0	-1666180	-7429301

APPENDIX II

MAP OF THE STUDIED CITY

The sources and sinks of Mesaieed industrial city, that are considered in this work, are represented in the map below. The locations of all the sources in addition to the methanol and urea sinks are determined using Google Earth Pro. However, algae, greenhouse, saline storage and EOR are potential sinks and they are not currently active. Therefore, their correspondent locations were not shown on the map.

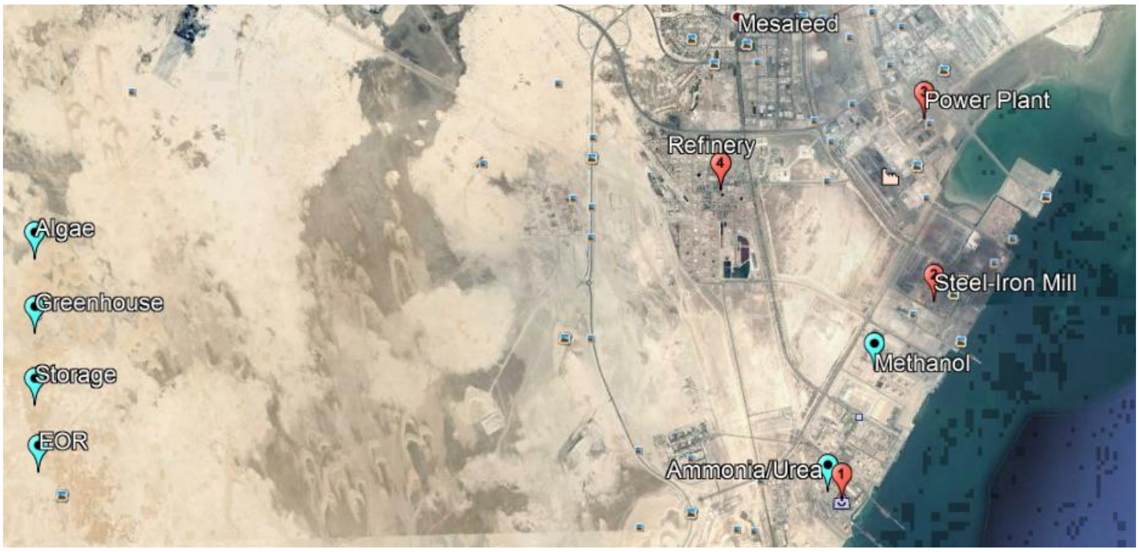

Figure 19: Mesaieed Industrial City Map

BIBLIOGRAPHY

BP Statistical Review of World Energy, 2017 [Online]. Available: http://www.bp.com/statisticalreview [Accessed 9 January 2018].

Lindo Systems, What'sBest! 15.0 - Excel Add-In for Linear, Nonlinear, and Integer Modeling and Optimization [Online]. Available: www.lindo.com [Accessed].

Preventing formation of hydrate plugs [Online]. Petrowiki. Available: http://petrowiki.org/Preventing_formation_of_hydrate_plugs [Accessed 13/1/2018].

US Fossil Fuels, 2016 [Online]. The National Academies of Sciences, Engineering and Medicine. Available: http://needtoknow.nas.edu/energy/energy-sources/fossil-fuels/ [Accessed 4 January 2018].

ABBAS, Z., MEZHER, T. & ABU-ZAHRA, M. R. 2013. CO2 purification. Part I: Purification requirement review and the selection of impurities deep removal technologies. *International journal of greenhouse gas control,* 16**,** 324-334.

AL-MOHANNADI, D. M., ABDULAZIZ, K., ALNOURI, S. Y. & LINKE, P. 2017. On the synthesis of carbon constrained natural gas monetization networks. *Journal of Cleaner Production,* 168**,** 735-745.

AL-MOHANNADI, D. M., ALNOURI, S. Y., BISHNU, S. K. & LINKE, P. 2016. Multi-period carbon integration. *Journal of cleaner production,* 136**,** 150-158.

AL-MOHANNADI, D. M. & LINKE, P. 2016. On the systematic carbon integration of industrial parks for climate footprint reduction. *Journal of Cleaner Production,* 112**,** 4053-4064.

AMAN, Z. M. & KOH, C. A. 2016. Interfacial phenomena in gas hydrate systems. *Chemical Society Reviews,* 45**,** 1678-1690.

ASPELUND, A. & JORDAL, K. 2007. Gas conditioning—the interface between CO2 capture and transport. *International Journal of Greenhouse Gas Control,* 1**,** 343-354.

ATKINS, M. J., MORRISON, A. S. & WALMSLEY, M. R. 2010. Carbon emissions pinch analysis (CEPA) for emissions reduction in the New Zealand electricity sector. *Applied Energy,* 87**,** 982-987.

BAVOH, C. B., LAL, B., KEONG, L. K., BINTI JASAMAI, M. & BINTI IDRESS, M. 2016. Synergic kinetic inhibition effect of EMIM-Cl+ PVP on CO2 hydrate formation. *Procedia engineering,* 148**,** 1232-1238.

BAVOH, C. B., PARTOON, B., LAL, B., GONFA, G., KHOR, S. F. & SHARIF, A. M. 2017. Inhibition effect of amino acids on carbon dioxide hydrate. *Chemical Engineering Science,* 171**,** 331-339.

BENSON, S., BENNACEUR, K., COOK, P., DAVISON, J., DE CONINCK, H., FARHAT, K., RAMIREZ, C., SIMBECK, D., SURLES, T. & VERMA, P. 2012. Carbon capture and storage. *Global Energy Assessment-Toward a Sustainable Future***,** 993.

BRINCKERHOFF, P. 2011. Accelerating the uptake of CCS: industrial use of captured carbon dioxide. *New York*.

BUIT, L., AHMAD, M., MALLON, W. & HAGE, F. 2011. CO2EuroPipe study of the occurrence of free water in dense phase CO2 transport. *Energy Procedia,* 4**,** 3056-3062.

CARROLL, J. J. 2003. Problem is the result of industry's move to use higher pressures. *Pipeline & gas journal,* 230**,** 60-61.

CHAE, S. H., KIM, S. H., YOON, S.-G. & PARK, S. 2010. Optimization of a waste heat utilization network in an eco-industrial park. *Applied Energy,* 87**,** 1978-1988.

CHAPEL, D. G., MARIZ, C. L. & ERNEST, J. Recovery of CO2 from flue gases: commercial trends. Canadian society of chemical engineers annual meeting, 1999.

DARBY, M. 2016. Six EU countries have already met their 2030 climate targets. Climate Home News.

DE VISSER, E., HENDRIKS, C., BARRIO, M., MOLNVIK, M. J., KOEIJER, G. D., LILJEMARK, S. & LE GALLO, Y. 2008. Dynamis CO2 quality recommendations. *International Journal of Greenhouse Gas Control,* 2**,** 478-484.

DONG, C., DONG, X., JIANG, Q., DONG, K. & LIU, G. 2018. What is the probability of achieving the carbon dioxide emission targets of the Paris Agreement? Evidence from the top ten emitters. *Science of The Total Environment,* 622**,** 1294-1303.

DUGSTAD, A. & HALSEID, M. Internal corrosion in dense phase CO2 transport pipelines-state of the art and the need for further R&D. CORROSION 2012, 2012. NACE International.

EUROPEAN COMMISSION. 2016. *EU Climate Action* [Online]. European Commission. Available: https://ec.europa.eu/clima/citizens/eu_en [Accessed 16/6/2017].

FURUBAYASHI, T. & NAKATA, T. 2018. Cost and CO2 reduction of biomass co-firing using waste wood biomass in Tohoku region, Japan. *Journal of Cleaner Production,* 174**,** 1044-1053.

GADALLA, M. A., OLUJIC, Z., JANSENS, P. J., JOBSON, M. & SMITH, R. 2005. Reducing CO2 emissions and energy consumption of heat-integrated distillation systems. *Environmental science & technology,* 39**,** 6860-6870.

ICIS. 2014. *Caprolactam prices, markets & analysis* [Online]. Available: https://www.icis.com/chemicals/caprolactam/ [Accessed 2017].

KARIMI, M., HILLESTAD, M. & SVENDSEN, H. F. 2012. Natural gas combined cycle power plant integrated to capture plant. *Energy & Fuels,* 26**,** 1805-1813.

KELLAND, M. A. 2006. History of the development of low dosage hydrate inhibitors. *Energy & Fuels,* 20**,** 825-847.

KELLAND, M. A., REYES, F. T. & TROVIK, K. W. 2013. Tris (dialkylamino) cyclopropenium chlorides: Tetrahydrofuran hydrate crystal growth inhibition and synergism with polyvinylcaprolactam as gas hydrate kinetic inhibitor. *Chemical engineering science,* 93**,** 423-428.

KEMPER, J., SUTHERLAND, L., WATT, J. & SANTOS, S. 2014. Evaluation and analysis of the performance of dehydration units for CO2 capture. *Energy Procedia,* 63**,** 7568-7584.

MCCOLLUM, D. L. & OGDEN, J. M. 2006. Techno-economic models for carbon dioxide compression, transport, and storage & correlations for estimating carbon dioxide density and viscosity. *Institute of Transportation Studies*.

METZ, B., DAVIDSON, O., DE CONINCK, H., LOOS, M. & MEYER, L. 2005. IPCC special report on carbon dioxide capture and storage. Intergovernmental Panel on Climate Change, Geneva (Switzerland). Working Group III.

MUNIR, S. M., MANAN, Z. A. & ALWI, S. R. W. 2012. Holistic carbon planning for industrial parks: a waste-to-resources process integration approach. *Journal of Cleaner Production*, 33**,** 74-85.

NØRSTEBØ, V. S., MIDTHUN, K. & BJØRKVOLL, T. 2012. Analysis of carbon capture in an industrial park—a case study. *International Journal of Greenhouse Gas Control,* 9**,** 52-61.

OLIVIER, J., JANSSENS-MAENHOUT, G., MUNTEAN, M. & PETERS, J. 2016. Trends in Global CO2 Emissions: 2016 Report.

OLVERA-MARTÍNEZ, M. E., MENDOZA-FLORES, J. & GENESCA, J. 2015. CO 2 corrosion control in steel pipelines. Influence of turbulent flow on the performance of corrosion inhibitors. *Journal of Loss Prevention in the Process Industries*, 35**,** 19-28.

OOI, R. E., FOO, D. C., TAN, R. R., NG, D. K. & SMITH, R. 2013. Carbon constrained energy planning (CCEP) for sustainable power generation sector with automated targeting model. *Industrial & Engineering Chemistry Research,* 52**,** 9889-9896.

PERRY, S., KLEMEŠ, J. & BULATOV, I. 2008. Integrating waste and renewable energy to reduce the carbon footprint of locally integrated energy sectors. *Energy,* 33**,** 1489-1497.

PORTER, R. T., FAIRWEATHER, M., POURKASHANIAN, M. & WOOLLEY, R. M. 2015. The range and level of impurities in CO 2 streams from different carbon capture sources. *International Journal of Greenhouse Gas Control,* 36**,** 161-174.

PRAH, B. & YUN, R. 2017. Heat transfer and flow characteristics of CO2-hydrate mixture in pipeline. *Energy Procedia,* 114**,** 6813-6823.

PRAH, B. & YUN, R. 2018. CO2 hydrate slurry transportation in carbon capture and storage. *Applied Thermal Engineering,* 128**,** 653-661.

REČKA, L. & ŠČASNÝ, M. 2018. Brown coal and nuclear energy deployment: Effects on fuel-mix, carbon targets, and external costs in the Czech Republic up to 2050. *Fuel,* 216**,** 494-502.

REICHE, D. 2010. Energy Policies of Gulf Cooperation Council (GCC) countries—possibilities and limitations of ecological modernization in rentier states. *Energy Policy,* 38**,** 2395-2403.

ROOSTA, H., DASHTI, A., MAZLOUMI, S. H. & VARAMINIAN, F. 2016. Inhibition properties of new amino acids for prevention of hydrate formation in carbon dioxide–water system: Experimental and modeling investigations. *Journal of Molecular Liquids,* 215**,** 656-663.

RUSHING, S. 2009. Examining CO2 Sources for Algae. *Biodiesel Magazine.*

SAID, Z., ALSHEHHI, A. A. & MEHMOOD, A. 2018. Predictions of UAE's renewable energy mix in 2030. *Renewable Energy,* 118**,** 779-789.

SHENOY, A. U. & SHENOY, U. V. 2012. Targeting and design of energy allocation networks with carbon capture and storage. *Chemical engineering science,* 68**,** 313-327.

SLOAN JR, E. D. & KOH, C. 2007. *Clathrate hydrates of natural gases,* CRC press.

SONGOLZADEH, M., SOLEIMANI, M., TAKHT RAVANCHI, M. & SONGOLZADEH, R. 2014. Carbon dioxide separation from flue gases: a technological review emphasizing reduction in greenhouse gas emissions. *The Scientific World Journal,* 2014.

STIJEPOVIC, M. Z. & LINKE, P. 2011. Optimal waste heat recovery and reuse in industrial zones. *Energy,* 36**,** 4019-4031.

TAN, R. R. & FOO, D. C. 2007. Pinch analysis approach to carbon-constrained energy sector planning. *Energy,* 32**,** 1422-1429.

UNDP. 2016. *Lebanon Climate Act: Engaging the Private Sector in Carbon Mitigation* [Online]. UNDP Lebanon. [Accessed 16/6/2017].

USSIRI, D. A. & LAL, R. 2017. Carbon Sequestration for Climate Change Mitigation and Adaptation. Springer.

VAN BEERS, D. 2006. Capturing regional synergies in the Kwinana industrial area. *Status Report*.

WORLD BANK 2016. *State and trends of carbon pricing 2016*, World Bank Publications.

WORLD DATA ATLAS. 2016. *Qatar-CO2 emissions per capita* [Online]. Knoema. Available: https://knoema.com/atlas/Qatar/CO2-emissions-per-capita [Accessed 28/12/2017].

XIANG, Y., WANG, Z., YANG, X., LI, Z. & NI, W. 2012. The upper limit of moisture content for supercritical CO 2 pipeline transport. *The Journal of Supercritical Fluids*, 67**,** 14-21.

YANG, M., SONG, Y., JIANG, L., ZHU, N., LIU, Y., ZHAO, Y., DOU, B. & LI, Q. 2013. CO2 hydrate formation and dissociation in cooled porous media: A potential technology for CO2 capture and storage. *Environmental science & technology*, 47**,** 9739-9746.

ZEVENHOVEN, R. & KILPINEN, P. 2001. *Control of pollutants in flue gases and fuel gases*, Helsinki University of Technology Espoo, Finland.

ZHANG, Y., WANG, D., YANG, J., TIAN, L. & WU, L. 2016. Research on the Hydrate Formation in the process of GasPhase CO2 Pipeline Transportation. *International Journal of Heat and Technology*, 34**,** 339-344.